Accepted Manuscript

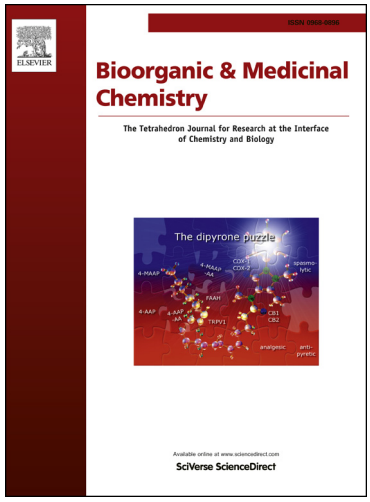

Curcumin-inspired cytotoxic 3,5-bis(arylmethylene)-1-(*N*-(*ortho*-substituted aryl)maleamoyl)-4-piperidones: A novel group of topoisomerase II alpha inhibitors

Amitabh Jha, Katherine M. Duffield, Matthew R. Ness, Sujatha Ravoori, Gabrielle Andrews, Khushwant S. Bhullar, H.P. Vasantha Rupasinghe, Jan Balzarini

PII: S0968-0896(15)30005-5
DOI: http://dx.doi.org/10.1016/j.bmc.2015.08.023
Reference: BMC 12527

To appear in: *Bioorganic & Medicinal Chemistry*

Received Date: 29 May 2015
Revised Date: 10 August 2015
Accepted Date: 20 August 2015

Please cite this article as: Jha, A., Duffield, K.M., Ness, M.R., Ravoori, S., Andrews, G., Bhullar, K.S., Vasantha Rupasinghe, H.P., Balzarini, J., Curcumin-inspired cytotoxic 3,5-bis(arylmethylene)-1-(*N*-(*ortho*-substituted aryl)maleamoyl)-4-piperidones: A novel group of topoisomerase II alpha inhibitors, *Bioorganic & Medicinal Chemistry* (2015), doi: http://dx.doi.org/10.1016/j.bmc.2015.08.023

Curcumin-inspired cytotoxic 3,5-bis(arylmethylene)-1-(*N*-(*ortho*-substituted aryl)maleamoyl)-4-piperidones: A novel group of topoisomerase II alpha inhibitors

Amitabh Jha,[a, *] Katherine M. Duffield,[a] Matthew R. Ness,[a] Sujatha Ravoori,[a] Gabrielle Andrews,[a] Khushwant S. Bhullar,[b] H.P. Vasantha Rupasinghe,[b] and Jan Balzarini[c]

[a] Department of Chemistry, Acadia University, Wolfville, NS, Canada

[b] Department of Environmental Sciences, Faculty of Agriculture, Dalhousie University, Truro, NS, Canada

[c] Rega Institute for Medical Research, KU Leuven, B-3000 Leuven, Belgium

ABSTRACT

Three series of novel 3,5-bis(arylmethylene)-1-(*N*-(*ortho*-substituted aryl)maleamoyl)-4-piperidones, designed as simplified analogs of curcumin with maleic diamide tether, were synthesized and bioevaluated. These compounds displayed potent cytotoxicity towards human Molt 4/C8 and CEM T-lymphocytes as well as murine L1210 leukemic cells. In contrast, the related *N*-arylmaleamic acids possessed little or no cytotoxicity in these three screens. Design of these compounds was based on molecular modeling studies performed on a related series of molecule in a previous study. Representative title compounds were found to be significantly potent in inhibiting the activity of topoisomerase II alpha indicating the possible mode of action of these compounds. These compounds were also potent antioxidants *in vitro* and attenuated the AAPH triggered peroxyl radical production in human fibroblasts. Various members of these series were also well tolerated in both *in vitro* and *in vivo* toxicity analysis.

Keywords: curcumin analogs; 4-piperidones; maleamic acids; cytostatic activity; QSAR; topoisomerase IIα inhibition.

[*] Corresponding author. Tel.: +1 902 585 1515; Fax +1 902 585 1414; E-mail: ajha@acadiau.ca.

1. Introduction

Curcumin (Figure 1) is a natural product isolated from *Curcuma longa*, commonly known as turmeric, one of the most commonly used spices worldwide [1]. Scientists have intensively studied this compound over the decades and a number of its pharmacological aspects such as anti-inflammatory, antitumor, anti-angiogenic, antioxidant, antibacterial, cardioprotective and neuroprotective properties have been documented [2-6]. More than one hundred clinical trials have been/are being conducted on this natural compound [7], including those for the treatment of metastatic breast cancer [8], colon cancer [9], advanced pancreatic cancer [10], cystic fibrosis [11], inflammatory bowel disease [12], and Alzheimer's disease [13]. As commonly observed in dietary phytochemicals, curcumin displays an excellent safety profile with negligible toxicological manifestations; however, its clinical efficacy is marred with its poor bioavailability which has prevented this molecule from culminating into an efficacious clinical drug [14].

Continuous efforts in our lab are focused on analogs of curcumin in attempts to develop molecules with superior pharmacodynamic and pharmacokinetic profile than those of curcumin [15-27]. Among our previous research, we have prepared and studied curcumin analogs where the diarylheptanoid skeleton of curcumin was retained (Series **1-3**, Fig. 1) [15-18]. These studies involved evaluation of anticancer, antioxidant, anti-hypertensive, and/or anti-HIV properties of these compounds. It was observed in these investigations [15-18] that compounds retaining the oxygenation pattern similar to that of curcumin were found to be more active in terms of their anticancer and antioxidant potency *in-vitro* compared to the other analogs. Simultaneously, we have also studied a large number of diarylpentanoids (Series **4-10**, Figure 1) [19-24], which may be viewed as simplified analogs of diarylheptanoid curcumin. Curcumin as well as its analogs (**1-10**) contain α,β-unsaturated carbonyl group(s) and therefore are Michael acceptors with selective affinity for protein thiols as opposed to O/N-based nuclephiles found on genetic materials [25, 28]. Notably, the analogs from series **5-10** contain additional enone moiety in their side chains bearing for interaction with auxiliary binding domain [20] and/or protein thiolation [25, 28].

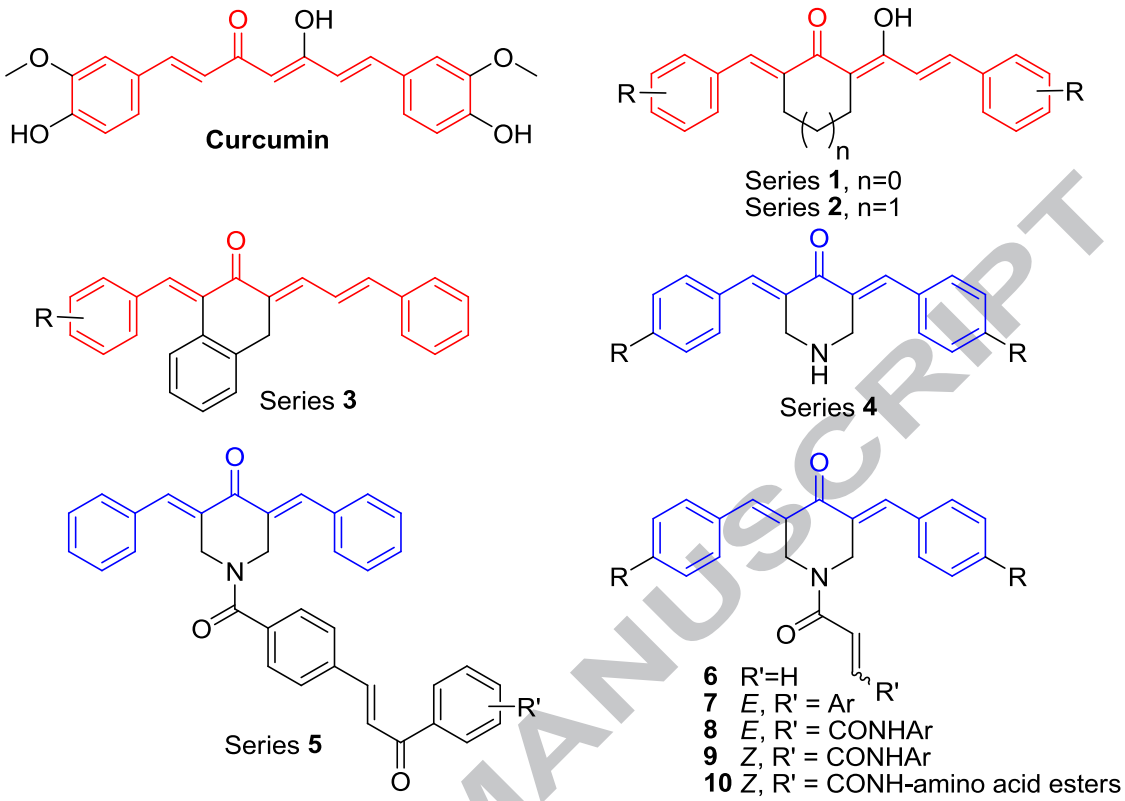

Figure 1: Molecular structures of curcumin and its previously studied analogs.

The parent diarylheptanoids, namely 3,5-bisarylmethylene-4-piperidones **4**, and their derivatives **(5-10)** (Figure 1) were consistently found to possess higher level of *in vitro* cytotoxicity than diarylheptanoids **1-3**. Most of these compounds displayed cytotoxicity in single digit to sub-micromolar inhibitory concentrations against the cancer cell lines tested.

We have identified human topoisomerase IIα as a potential molecular target for 3,5-bisarylmethylene-4-piperidone derivatives [22]. This thiol-rich enzyme is essential for sustained cell proliferation [29-31]. This enzyme releases torsional strain in DNA double helical structure through transient double strand breaks facilitating segregation of the strands, allowing replication and transcription processes to occur [32]. Catalytic inhibition of these processes halts replication and transcription, eventually arresting the cell growth. Also, if the enzyme inhibition occurs by poisoning, the nicks in the DNA strands created by the enzyme cannot re-ligate resulting in lethal lesions in the DNA frame work, which then leads to apoptosis [29, 30]. Since the expression of

topoisomerase IIα is amplified in cancerous cells, targeting this enzyme by protein-thiolators thus offers a viable pathway of selectivity targeting malignancies.

Of a particular relevance to this report are series **9** compounds ((*Z*)-4-((3*E*,5*E*)-3,5-bisbenzylidene-4-oxopiperidin-1-yl)-*N*-aryl-4-oxobut-2-enamides, Figure 1) where substituted anilines were conjugated to the parent 3,5-bisarylmethylene-4-piperidones via maleamic diamide moiety [21]. The rationale behind their design was as follows: a) incorporation of an additional enone functionality terminating with an aryl carbomoyl group (as opposed to a proton) that will elicit higher electrophilicity to the enone towards thiol group than the corresponding unsubstituted acryloyl group; b) the placement of different substituents on the aryl ring adjacent to carbomoyl group would further alter the polarity of the enone functionality; and c) the *Z*-geometry of the maleamic diamide moiety will offer minimum impedance to the approach of the cellular thiol. All compounds of series **9** were found to show remarkable *in vitro* cytostatic activity; the most active of them all was found to be (*Z*)-4-((3*E*,5*E*)-3,5-dibenzylidene-4-oxopiperidin-1-yl)-*N*-(2,6-dimethylphenyl)-4-oxobut-2-enamide with sub-micromolar IC_{50} towards three out of four representative cancer cell lines tested. Among tested compounds, this was the only compound with *ortho*- substitutions on the aniline ring [21]. As a guided amplification of this project, we decided to synthesize a larger library of series **9**-type compounds with *ortho*- substituents on the aniline ring. The designed compounds for this investigation can be broadly classified into three series (**9Aa-i**, **9Ba-i** and **9Ca-i; Scheme 1**) based on substitution on the aryl ring (unsubstituted, 4-nitro- and 4-carboethoxy-) of the 3,5-bisarylmethylene-4-piperidone moiety. Since these compounds are predicted to act, at least in part, *via* protein thiolation, electron withdrawing groups like 4-nitro- and 4-carboethoxy- on the arylmethylene moiety should impart higher electrophilicity to the enone system towards protein thiolation in comparison to the corresponding phenylmethylene analogs. Overall, this study was conducted with the aim of assessing the anti-cancer activity of these novel compounds in comparison to parent molecules along with other concomitant pharmacological properties. We herein report potent cytostatic, antioxidant, human topoisomerase IIα inhibitory activities and toxicity of 27 such compounds.

2. Results and discussion

2.1. Chemistry

Synthesis of series **9** compounds was accomplished by following previously reported procedure [23]. Reaction of 4-piperidone hydrate hydrochloride with two equivalents of aromatic aldehydes (benzaldehyde, 4-nitrobenzaldehyde and 4-carboethoxybenzaldehyde) in acetic acid under the influence of dry HCl gas resulted in formation of 3,5-diarylmethylenepiperidone acid salts (**4A-C**) as bright yellow or orange precipitate. These compounds were then individually reacted with acryloyl chloride under basic conditions to produce compounds **6A-C**. Maleanilinic acids **11a-i** were synthesized by reacting maleic anhydride with corresponding substituted anilines in dichloromethane. Maleanilinic acids **11a-i** were activated by reacting them with ethyl chloroformate, and triethylamine in THF. To these solutions, compounds **4A**, **4B** and **4C** were then individually added to yield compounds of series **9A**, **9B** and **9C**, respectively (Scheme 1). All products were purified by digestion in methanol or by column chromatography and were then completely characterized by spectroscopic means. Compounds **6C**, **9Aa-f**,**h**,**i**, **9Ba-i** and **9Ca-i** are new to the chemical literature. Based on spectroscopic data, the double bond geometry across the dibenzylidene system was found to be *E*, and that across maleic diamide was found to be *Z*, as expected [21]. It was interesting to note that all compounds of series **9** showed more peaks in the ^{13}C NMR spectra than expected based on C2 symmetry in the molecule along piperidone >C=O and N axis. We have observed this phenomenon previously [33]. It meant that these compounds predominantly occupy a non-symmetrical conformation due to the electron delocalization on piperidone amide.

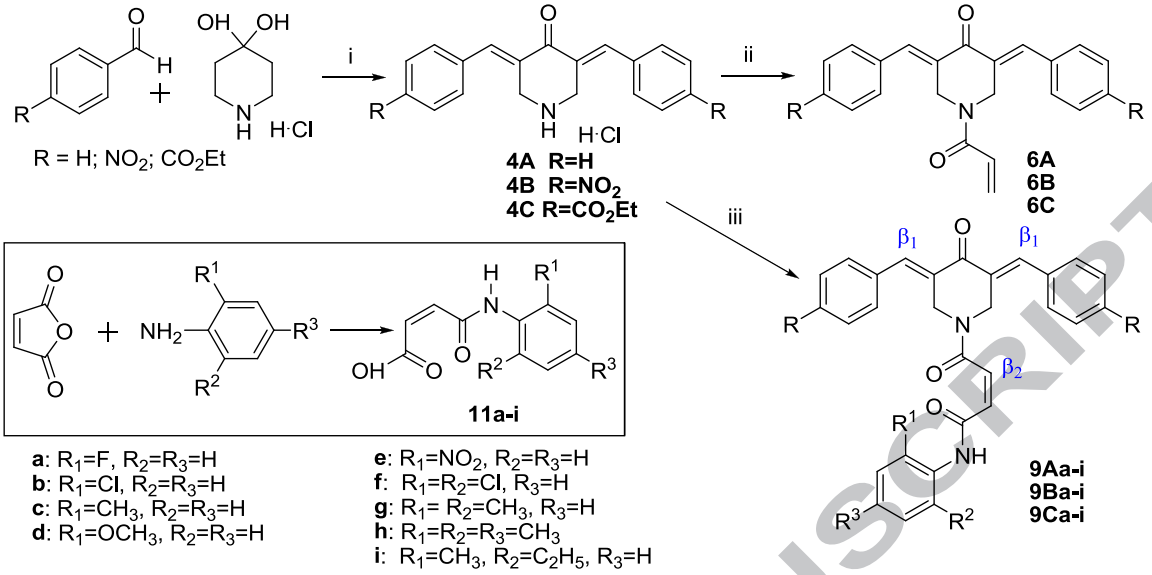

Scheme 1: Synthetic routes for the preparation of series **4**, **6**, **9** and **11** compounds. Conditions: (i) HCl, AcOH; (ii) $ClCOCH=CH_2$, $N(C_2H_5)_3$, DCM; (iii) $N(C_2H_5)_3$, $ClCOOC_2H_5$/**11a-i**, THF.

2.2. Biological evaluations

2.2.1. Cytostatic activity

First, the cytostatic activities of compounds **4C**, **6C**, **9Aa-i**, **9Ba-i**, **9Ca-i** and **11a-i** were evaluated against human CD_4^+ T-lymphocyte Molt4/C8 and CEM cells as well as murine L1210 lymphocytic leukemia cells following a literature procedure [34]. The results are presented in Table 1 in four different groups for comparison purposes: 1) **Group A**: 3,5-diphenylmethylene-4-piperidone (**4A**) and its derivatives (**6A**, **9Aa-i**); 2) **Group B**: 3,5-di(4-nitrophenylmethylene)-4-piperidone (**4B**) and its derivatives (**6B**, **9Ba-i**); 3) **Group C**: 3,5-di(4-carboethoxyphenylmethylene)-4-piperidone (**4C**) and its derivatives (**6C**, **9Ca-i**); and 4) **Group D**: substituted maleanilinic acids (**11a-i**). Clinical anticancer drug melphalan (alkylating agent) and curcumin were used as reference drugs.

With regards to the cytostatic activity, a few general observations will be stated first. It is clearly evident from the data in Table 1 that nearly all the compounds tested against three representative cancer cell lines are potent anticancer agents as well as promising lead molecules for further development. Baring the parent compounds **4A-C**, all the other compounds tested have shown superior cytostatic activity than melphalan and curcumin against each of the cancer cell lines. Approximately 75% of the IC_{50} data reported in Table 1 are in submicromolar range. Human T-lymphocyte CEM cells turned

out to be the most sensitive cell line to the tested compounds (average IC_{50} 0.27 μM for series **9** compounds) while the least sensitive of the three was murine leukemic L1210 cells (average IC_{50} 2.14 μM for series **9** compounds). Among the three groups, group **B** compounds with **4B** (R=NO_2) as parent molecule emerged as most potent (average IC_{50} 0.29 μM for three cell lines) but least selective (average selectivity ratio SI 2.6) series of molecules. By the same token, group **C** compounds with **4C** (R=CO_2Et) as parent molecule came out as most selective with average SI value of 15.3 and displayed remarkably high potency against CEM cells (average IC_{50} 0.17 μM). These observations support the assertion that electron withdrawing groups on the aryl ring (e.g. 4-NO_2 on **4B** and 4-CO_2Et on **4C**) improve the cytostatic activity presumably by increasing the electrophilicity of the enone functionality towards cellular nucleophiles. Considering all data reported in Table 1, compound **9Cb**, formed by conjugation of **4C** and **11b**, showed the lowest IC_{50} value of 89 nM against CEM cells.

Compounds **6A-C**, the acryloyl amides of **4A-C**, showed marked improvement in their cytostatic activity as compared to their parent molecule, especially in group **B** and **C** (Table 1). This gives confidence to the hypothesis that incorporation of an additional enone functionality in the molecules improves the cytostatic activity. However, with the replacement of one of the hydrogens from the terminal position of acryloyl group with *N*-arylcarbamoyl group imparting *Z* geometry to the double bond (series **9A-C** compounds) has led to further increase in the cytostatic potential in most cases. As mentioned earlier, series **9A-C** were designed to include *ortho*-substituents on the arylamine rings as such a modification appeared to improve the anticancer potential [21]. When the cytostatic activities of series **9A** is compared to that of series **9** compounds previously reported with no, *meta*- and/or *para*-substitution(s) on the arylamine rings [21], a significant improvement in the cytostatic activity was noticed. This gives positive support to our hypothesis. As the *ortho*- substituents are known to impart electronic as well as steric effects on the molecule, it is believed that the 3D topology of the resulting molecules is significantly altered leading to better binding with the molecular target. This will be discussed further in the QSAR section. Compounds of series **9** can be viewed as diamides of maleic acid. One may argue that their cytostatic activity could be due to two electrophilic molecules (the parent **4** and the corresponding *N*-arylmaleamic acid **11**)

after the hydrolysis of the amide at the piperidyl nitrogen atom. This seems highly unlikely for the following reasons. First, most of the series **9** compounds are significantly more potent than the parent molecule **4**. Secondly, the data in Table 1 reveals that *N*-arylmaleamic acids **11a-i** (Group **D**) are essentially inactive as cytostatic agents (IC_{50} value > 100 μM in all cases). Encouraged by these results, compounds **9Aa, 9Ad and 9Af** were also evaluated against NCI's 56 human tumor cell lines representing nine different neoplastic conditions, namely breast, central nervous system, colon, leukemia, melanoma, non-small cell lung, ovarian, prostate and renal [35]. The data generated are summarized in Table 2.

Table 1. Evaluation of compounds from series **4**, **6**, **9** and **11** against human Molt-4/C8 and CEM T-lymphocytes and murine L1210 leukemic cells

	IC_{50} (μM)			
Compound	Molt 4/C8	CEM/0	L1210	SR[a]
4A[b]	1.67±0.15	1.70±0.02	7.96±0.11	4.8
6A[b]	1.42±0.27	1.48±0.34	8.69±0.73	6.1
9Aa	0.53±0.18	0.48±0.07	2.1±0.3	4.9
9Ab	0.82±0.56	0.59±0.22	4.1±3.0	6.9
9Ac	0.42±0.13	0.46±0.06	4.4±3.0	10.5
9Ad	0.43±0.05	0.42±0.01	1.7±0.1	4.0
9Ae	0.90±0.63	0.54±0.18	3.6±0.6	6.7
9Af	0.44±0.06	0.40±0.01	1.9±0.1	4.8
9Ag	0.40±0.04	0.39±0.05	4.2±2.8	10.8
9Ah	0.44±0.05	0.42±0.03	2.2±0.3	5.2
9Ai	0.43±0.07	0.37±0.06	4.0±2.4	10.8
4B[b]	8.28±0.75	4.47±2.28	32.9±4.2	7.4
6B[b]	0.15±0.06	0.26±0.02	0.42±0.07	2.8
9Ba	0.12±0.06	0.14±0.09	0.36±0.03	3.0
9Bb	0.27±0.02	0.23±0.20	0.38±0.02	1.4
9Bc	0.26±0.15	0.22±0.20	0.41±0.04	1.9
9Bd	0.27±0.13	0.15±0.09	0.33±0.05	2.2
9Be	0.37±0.05	0.37±0.07	1.1±0.6	3.0
9Bf	0.28±0.09	0.18±0.12	0.36±0.00	2.0
9Bg	0.21±0.13	0.11±0.05	0.35±0.01	3.2
9Bh	0.15±0.06	0.10±0.04	0.39±0.01	3.9
9Bi	0.19±0.08	0.12±0.07	0.33±0.05	2.8
4C	1.1±0.7	1.0±0.7	6.9±0.5	6.9
6C	0.35±0.06	0.16±0.02	1.7±0.07	10.6
9Ca	1.5±1.1	0.30±0.05	8.1±0.8	27.0
9Cb	0.59±0.38	0.089±0.061	1.7±0.1	19.1
9Cc	0.67±0.40	0.11±0.05	1.7±0.1	15.5
9Cd	0.36±0.08	0.12±0.09	1.6±0.1	9.2
9Ce	0.29±0.03	0.12±0.01	1.1±0.1	13.3
9Cf	1.1±0.6	0.22±0.19	5.0±1.2	22.7
9Cg	0.95±0.47	0.28±0.17	3.5±1.3	12.5
9Ch	0.67±0.39	0.16±0.13	2.5±0.9	15.6

9Ci	0.95±0.47	0.28±0.17	3.5±1.3	12.5
11a	365±0	480±29	333±13	NC[c]
11b	228±27	279±3	251±23	NC
11c	>500	>500	>500	NC
11d	134±23	189±10	100±2	NC
11e	353±6	426±28	395±22	NC
11f	>500	>500	>500	NC
11g	>500	>500	>500	NC
11h	>500	>500	>500	NC
11i	>500	>500	>500	NC
Melphalan	3.24±0.79	2.6±1.2	5.8±0.3	3.9
Curcumin	9.0±1.9	15 ± 5	22 ± 1	2.4

[a] SR indicates the selectivity ratio, i.e., the ratio between the highest and lowest IC_{50} values of either the T-lymphocytes or murine leukemic cells.
[b] Reprinted in part from literature [36].
[c] NC: Not calculated.

The results shown in Table 2 demonstrate that when all cell lines are considered, each of the series **9A** compounds tested are significantly more cytostatic than melphalan and curcumin. An essential characteristic of a potential anticancer drug is selective toxicity for certain tumor cell types rather than them being indiscriminately cytostatic. The selectivity index (SI) values for compounds **9Aa**, **9Ad** and **9Af** for all the tumor cell lines reveal their wide differential sensitivity towards human tumor cell types; each of these compounds boasted impressive selectivity (SI for **9Aa**: >3236; SI for **9Ad**: >1738; SI for **9Af**: 1318). A comparative review of the GI_{50} values with respect to various cell line classes in Table 2 revealed that each of these three compounds exerted greater toxicity against leukemic, colon and prostate cancer cell lines than against those representing other cancers. Even among leukemic cell lines, compounds **9Aa** and **9Ad** show GI_{50} in low nM range (60 and 20 nM respectively). Melphalan is used in combination chemotherapy to treat chronic leukemias along with wide range of other malignancies [37]. The results in Table 2 indicate that **9Aa** and **9Ad** are respectively, 93 and 280 times more potent than melphalan against the leukemic cell lines *in vitro*. The novel findings that the compounds possess significant potencies and preferential cytotoxicity for certain tumor cells suggests that compounds of series **9** studied here are promising candidate anticancer agents with selective toxicity.

Table 2. Evaluation of compounds **9Aa**, **9Ad** and **9Af** and reference compounds against a panel of human tumor cell lines

Cell lines	No.[a]		**9Aa**	**9Ad**	**9Af**	Melphalan[d]	Curcumin[e]
Leukemia	3	GI_{50} (μM)[b]	0.06	0.02	0.24	5.6	3.7
Lung cancer	9	GI_{50} (μM)	6.61	3.70	1.80	25.6	9.2
Colon cancer	7	GI_{50} (μM)	2.04	0.67	0.43	48.9	4.7
CNS cancer	6	GI_{50} (μM)	3.86	2.00	1.30	27.4	5.8
Melanoma	9	GI_{50} (μM)	3.60	1.60	1.20	33.0	5.9
Ovarian cancer	7	GI_{50} (μM)	5.66	3.30	1.40	41.1	9.1
Renal cancer	8	GI_{50} (μM)	2.97	2.30	1.70	32.2	8.9
Prostate cancer	2	GI_{50} (μM)	2.40	0.63	0.30	35.5	11.2
Breast cancer	5	GI_{50} (μM)	4.43	1.50	0.88	33.5	8.1
All cell lines	56	GI_{50} (μM)	**2.47**	**1.20**	**1.00**	**24.6**	**6.7**
		SI[c]	>3236	>1738	1318	79	10

[a] Number of individual cells lines tested representing the respective type of cancer.
[c] SI refers to the selectivity index. The SI figures for all cell lines were obtained by dividing the GI_{50} values of the least and most sensitive cells.
[d] GI_{50} values for melphalan were obtained from online NCI database (COMPARE data vector search, compound ID NSC 8806).
[e] GI_{50} values for curcumin were obtained from online NCI database (COMPARE data vector search, compound ID NSC 32982).

2.2.2. Topoisomerase IIα inhibitory activity

Human topoisomerase IIα (topo IIα) has been validated as a clinically important target for cancer drug development as it is a vital for chromosome segregation and cell division in cancer cells [38]. Multiple topo IIα inhibitors have been developed as antitumor agents and are already in clinical use for decades. The series of compounds **4A-C, 6A-C, 9Aa-i**, **9Ba-i** and **9Ca-i** containing a pharmacophore similar to curcumin in the current investigation were found to inhibit human topo IIα activity. Topo IIα inhibition assays were performed using a commercial human DNA topoisomerase IIα inhibition kit, according to the manufacturer's instructions (Topogen Inc, Columbus, OH). A representative gel picture displaying the topoisomerase IIα inhibition potential of the compounds **4A-C, 6A-C, 9Aa-i**, **9Ba-i** and **9Ca-i** is presented in Figure 2 A-C. Etoposide, sorafenib and cisplatin were used as reference drugs. Sorafenib, a multi-target kinase inhibitor, is also known to inhibit topoisomerase IIα in-vitro [39, 40] and in-vivo [41]. The results from this evaluation showed that all the assayed compounds, including

reference drugs (50 μM), exhibited strong inhibitory activity towards topo IIα *in vitro*. The gel analysis showed that most compounds displayed a weak linear DNA band in gel, thus exhibiting characteristics of interfacial topoisomerase poisons. Other compounds exhibited catalytic inhibition of topo IIα *in vitro*. Additionally, the topo IIα inhibitory effects of compounds **9Ad-9Ai, 4B, 6B** were much stronger than the other compounds, and that of the etoposide and the standard drugs at 50 μM concentrations. However, compounds **9Cc-9Ch** displayed a catalytic inhibitory activity as they blocked the activity of topo IIα directly (no relaxed DNA but strong supercoiled plasmid, Fig. 2C). Overall, the results revealed that all the tested compounds exhibited concrete influence on topo IIα activity at low concentrations. In summary, we established that the compounds **4A-C, 6A-C, 9Aa-i**, **9Ba-i** and **9Ca-i** demonstrated anticancer activity through the check on topo IIα activity, possibly by weakening the enzyme activity via excessive supercoiling, which proved detrimental for cancer cell proliferation.

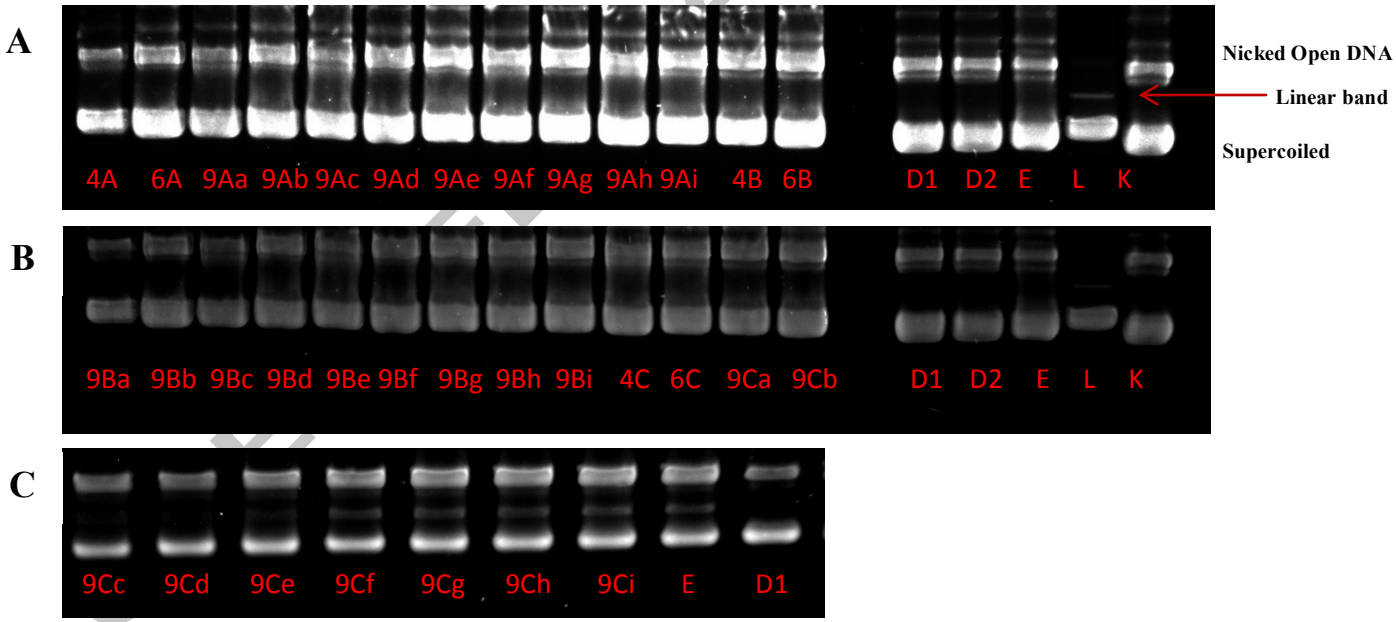

Figure 2. Topo IIα inhibitory activities of 3,5-bis(arylmethylene)-1-(*N*-arylmaleamoyl)-4-piperidones and related compounds. (**A**) The compounds were examined in a final concentration of 50 μM, respectively, as designated. Lanes **4A-6B**: pHOT1 DNA + 4 U topo IIα + test compounds in designated concentrations; Lane D1: pHOT1 DNA+ 4 U topo IIα + sorafenib; Lane D2: pHOT1 DNA + 4 U topo IIα + cisplatin; Lane E: pHOT1 DNA + 4 U topoII + etoposide; Lane L: Marker DNA, Linear pHOT1, Lane K: pHOT1 DNA, supercoiled. (**B**) The compounds were examined in a final concentration of 50 μM, respectively, as designated. Lanes **9Ba-9Cb**: pHOT1 DNA + 4 U topo IIα + test

compounds in described concentrations; Lane D1: pHOT1 DNA+ 4 U topo IIα + sorafenib; Lane D2: pHOT1 DNA + 4 U topo IIα + cisplatin; Lane E: pHOT1 DNA + 4 U topoII + etoposide; Lane L: Marker DNA, Linear pHOT1, Lane K: pHOT1 DNA, supercoiled. (**C**) The compounds were examined in a final concentration of 50 μM, respectively, as designated. Lanes **9Cc-9Ci**: pHOT1 DNA + 4 U topo IIα + test compounds in described concentrations; Lane E: pHOT1 DNA + 4 U topoII + etoposide; Lane D1: pHOT1 DNA + 4 U topo IIα + sorafenib.

2.2.3. Anti-oxidant activity

In order to evaluate compounds **4A-C, 6A-C, 9Aa-i**, **9Ba-i** and **9Ca-i** as potential anti-oxidant agents, we conducted *in vitro* tests using four antioxidant assays, viz. FRAP (ferric-reducing ability of plasma), ORAC (oxygen radical absorbance capacity), DPPH (2,2-diphenylpicrylhydrazyl anti-radical assay) and Cell-ROS assay (cellular reactive oxygen species detection assay) as described in experimental section below. Table 3 summarizes the anti-oxidant and cytoprotective activity data obtained for these 33 compounds as well as curcumin at 100 μM concentrations. As observed before [33], curcumin exhibited the highest antioxidant activity in all the four antioxidants assays conducted *in vitro* ($p \leq 0.05$).

According to the FRAP assay results, all of the assayed compounds displayed active FRAP activity and none of the compounds failed the FRAP activity test. Among the synthesized compounds, **9Aa** (476.8 μM TE/L) showed the strongest *in-vitro* antioxidant activity in comparison to the other compounds ($p \leq 0.05$). Still, compared to curcumin, ~3-fold lower anti-oxidant activity was exhibited by compound **9Aa** *in vitro*. It was closely followed by compounds **9Ab-9Ae** in their ability to reduce ferric-tripyridyltriazine (Fe^{3+}-TPTZ) to its blue, ferrous form (Fe^{2+}-TPTZ). On the contrary, compound **4B** exhibited the weakest anti-oxidant activity (19.2 μM TE/L) while the compounds **4A** (34.3 μM TE/L) and **9Bg** (53.8 μM TE/L) closely preceded compound **4B** in their *in vitro* anti-oxidant potential ($p \leq 0.05$). It was also observed that anti-oxidant activities of the compounds **9Bd** and **9Cf** were ~three-fold weaker in comparison to the active compound **9Aa** ($p \leq 0.05$). Overall, the derivatives of the parent molecules indicated stronger antioxidant activities, which indicate the positive influence of structural modification on the biological properties of the compounds. The presence of higher number of phenyl ring in compounds 9**Aa** improved its antioxidant activity in comparison to the precursor molecule **4A**. The peroxyl radical scavenging activities of

these compounds were also assessed by the ORAC assay using fluorescence as the fluorophore, while curcumin was used as the reference index. Curcumin remained the strongest inhibitor of fluorescence degradation by APPH injury in ORAC assay *in vitro*. Interestingly, compounds **9Ad** and **9Ae**, which exhibited strong activity in FRAP analysis, likewise displayed the strongest ORAC activity (215.3-222.9 μM TE/L) in comparison to other compounds *in vitro* ($p \leq 0.05$). These were followed by compounds **9Cc**, **6A**, **9Ac**, **9Ba**, **9Bh** and **9Cb** ($p \leq 0.05$), which previously indicated active antioxidant capacity in the FRAP analysis. Similar to the FRAP analysis, **9Bg** demonstrated the weakest antioxidant activity *in vitro* ($p \leq 0.05$). Conversely, weak FRAP based anti-oxidant candidates like compounds **4A** and **4B** displayed much stronger anti-oxidant potential in ORAC analysis ($p \leq 0.05$); on the other hand, in the same comparison, compound **9Ai** lost about 3-folds of its anti-oxidant potential *in vitro*. However, the remaining compounds displayed similar anti-oxidant capacity to FRAP analysis *in vitro* ($p \leq 0.05$). These results also supported the effect of structural modification as discussed in FRAP analysis, particularly the compounds **9Ad** and **9Ae** with unique substituents at positions 2 (R1= OCH_3 and NO_2) and/or 6 (R2=H).

Additionally, the *in vitro* anti-oxidant activity of these compounds was also determined by using the 2,2-diphenyl-1-picrylhydrazyl (DPPH) assay (Table 3), which estimates anti-oxidant activity by HAT mechanism. The compounds **9Bd** and **9Bf** exhibited the strongest anti-radical scavenging activity, analogous to curcumin *in vitro* ($p \leq 0.05$). The structure of these compounds was similar to **9Ad** and **9Ae** with similarly substituents at positions 2 (R1= OCH_3 and Cl) and/or 6 (R2=H). Likewise, assay of compound **9Ae** resulted in the smallest DPPH radical trapping potential, also in line with FRAP results, but in contradiction with ORAC analysis *in vitro* ($p \leq 0.05$). Finally, the ability of the test compounds to inhibit production of cellular ROS was assessed in a WI-38 cell model system. The results showed that the strongest peroxyl radical scavenging activity was displayed by compounds **9Bf**, **9Bi** and **9Ce** *in vitro* ($p \leq 0.05$). These top antioxidants were closely followed by multiple compounds in the ranges **9Be-i** and **9Ca-g**, thus demonstrating strong cytoprotective activities of these series of assayed compounds *in vitro* ($p \leq 0.05$). Weak ROS inhibitory activity was exhibited by compounds of series **9A** and compounds **9Ch** and **9Ci**, which showed ~half cytoprotective ability

compared to curcumin *in vitro* ($p \leq 0.05$). Such results can be related to the presence of CH_3 as key substituent substitutions at positions 2 (R1) and/or 6 (R2) in these compounds. For compounds **9Aa**, **9Ad**, **9Ae** and **9Bd**, which topped the antioxidant activity charts, their ROS scavenging ability was frail in cytoprotection analysis *in vitro* ($p \leq 0.05$). Overall, the ROS inhibition results were generally similar to FRAP and DPPH analysis with the exceptions of compounds **9Ae**, **9Ag**, **9Ah** and **9Bc**, which showed <50% ROS inhibition *in vitro*. In summary, many compounds of these series were active antioxidants but curcumin remained the strongest antioxidant compound in the current investigation.

Table 3. Antioxidant activity evaluation of 3,5-bis(arylmethylene)-1-(*N*-arylmaleamoyl)-4-piperidones (**4A-C**, **6A-C**, **9Aa-i**, **9Ba-i** and **9Ca-i**) and cytoprotective agents under four assay systems.

Compound	FRAP (μM TE/L)	ORAC (μM TE/L)	DPPH (% inhibition)	ROS (% inhibition)
4A	34.3±2.3^{pq}	92.7±1.9^{ijkl}	52.5±2.6^{op}	63.6±2.5^{cdefg}
6A	149.2±5.7^{kl}	181.7±7.3^{bc}	62.4±4.1^{jklmn}	56.4±1.5^{fghi}
9Aa	476.8±6.8^{a}	116.5±4.8^{fghij}	52.3±2.3^{op}	58.2±0.9^{efgh}
9Ab	444.3±12.0^{b}	134.6±3.3^{def}	53.3±1.0^{op}	54.9±3.5^{fghij}
9Ac	432.4±13.2^{b}	173.7±4.5^{bc}	60.4±2.7^{lmno}	52.2±2.9^{hij}
9Ad	434.5±11.1^{b}	222.9±2.2^{a}	54.9±1.8^{nop}	54.5±0.8^{ghij}
9Ae	441.4±4.5^{b}	215.3±6.4^{a}	49.5±2.8^{p}	49.5±0.4^{hij}
9Af	202.6±4.6^{ij}	120.8±14.6^{efghi}	69.1±3.3^{hijk}	51.4±2.4^{hij}
9Ag	277.1±3.0^{e}	161.8±9.4^{bcd}	68.4±3.0^{hijkl}	48.3±1.6^{ij}
9Ah	259.7±2.6^{ef}	115.7±7.7^{fghijk}	82.8±2.0^{cde}	49.7±2.9^{hij}
9Ai	302.1±5.7^{d}	88.1±4.7^{jklm}	78.6±1.3^{defg}	51.4±1.2^{hij}
4B	19.2±1.4^{q}	104.2±3.6^{fghijk}	76.1±2.6^{efgh}	64.1±3.6^{cdef}
6B	121.7±4.5^{mn}	95.3±2.0^{hijkl}	76.4±4.6^{efgh}	61.7±2.3^{defg}
9Ba	232.3±3.4^{gh}	176.0±5.3^{bc}	68.2±3.4^{hijklm}	65.9±2.6^{bcde}
9Bb	134.8±5.3^{lmn}	92.9±4.5^{ijkl}	87.1±2.6^{bc}	65.6±2.8^{bcde}
9Bc	195.8±2.7^{j}	92.3±4.1^{ijkl}	85.6±0.7^{bcd}	63.5±0.4^{cdefg}
9Bd	100.8±2.3^{o}	70.10±3.2^{lm}	96.8±1.5^{a}	69.1±2.4^{cbcd}
9Be	120.5±2.4^{mno}	105.6±6.6^{fghijk}	81.8±0.7^{cde}	71.4±4.1^{abc}
9Bf	140.5±5.8^{klm}	68.3±0.8^{lm}	92.2±1.2^{ab}	77.7±4.7^{a}
9Bg	53. 8±4.8^{p}	60.5±5.4^{m}	86.8±1.6^{bc}	71.1±0.7^{abc}
9Bh	245.4±7.4^{fg}	177.9±11.0^{bc}	82.8±3.5^{cde}	69.1±0.4^{abcd}
9Bi	153.7±4.4^{kl}	128.7±8.8^{efg}	80.6±1.9^{cdef}	77.9±4.2^{a}
4C	160.7±2.9^{k}	67.1±5.8^{lm}	68.6±1.8^{hijkl}	73.9±5.9^{ab}
6C	208.5±3.6^{ij}	150.4±8.0^{cde}	54.7±2.0^{nop}	70.8±2.7^{abcd}
9Ca	317.3±8.6^{d}	180.5±16.5^{bc}	59.1±1.1^{mno}	69.1±2.6^{abcd}
9Cb	191.3±8.8^{j}	124.2±10.9^{egfhi}	68.4±1.2^{hijklm}	69.7±4.6^{abcd}
9Cc	347.8±5.5^{c}	191.4±9.8^{ab}	57.5±3.9^{nop}	67.8±3.6^{bcd}
9Cd	239.9±3.8^{fgh}	119.1±2.1^{efghi}	66.8±5.2^{ijklm}	67.3±2.2^{bcde}

9Ce	305.1±9.7^{d}	121.1±10.1^{efghi}	56.6±2.0^{nop}	77.7±4.5^{a}
9Cf	115.7±8.6^{no}	73.8±4.4^{klm}	70.7±2.8^{ghij}	72.6±2.3^{abc}
9Cg	220.9±4.8^{hi}	125.9±4.3^{efgh}	60.7±2.4^{klmno}	69.6±1.2^{abcd}
9Ch	245.1±6.7^{fg}	97.1±6.4^{ghijkl}	71.4±1.3^{ghi}	46.9±1.5^{j}
9Ci	251.5±3.6^{fg}	66.9±8.3^{lm}	72.1±3.5^{fghi}	47.2±0.2^{j}
Curcumin	1201.4±0.2	1581.9±28.4	96.8±1.3	98.7±0.4

Means ± standard deviation, followed by the different superscripted letters (a through q) within column are significantly different, Tukey's multiple means comparison test, $p \leq 0.05$). The compounds were assayed at 100 μM concentration.

2.2.4. In-vitro toxicology analysis

The *in vitro* cell culture model was used to screen the test compounds based on their toxicity by assessing parameters such as cell viability and membrane damage, succeeding incubation with the compounds for 12 h. These parameters were assessed by the MTS cell viability and LDH cytotoxicity assays (Table 4), based on measuring the reduction of tetrazolium to colored formazan, indicating the toxicity status. In line with the voluminous literature, curcumin emerged as the safest tested compound with minimal toxicological manifestations in the current study as well. Compounds **4A-C, 6A-C, 9Aa-i**, **9Ba-i** and **9Ca-i**, at the assayed concentration (100 μM) showed very low cytotoxic activity in human fibroblasts, with an average cell survival >80% compared to a vehicle control. However, among the tested compounds, compound **4B** was the least innocuous compound and exhibited highest toxicity to normal cells, as indicated by both MTS and LDH assays *in vitro* ($p \leq 0.05$). **4B** with highly electron withdrawing nature is the precursor of the series and non-toxic manifestation of its derivatives indicated that the modification of the compounds not only improved the cytostatic activity but augmented the safety profile as well. Interestingly, compound **4B** was also the weakest antioxidant candidate in the FRAP analysis as well indicating its electron withdrawing nature ($p \leq 0.05$). Following curcumin, the compounds **9Ad**, **9Ag**, **9Bb**, **9Bc**, **9Cd** and **9Ch** were less deleterious, as the average cellular viability of fibroblasts in their presence was >90% *in vitro*. These compounds were safer than their precursor molecule and the presence of phenyl ring substitutions at positions 2 (R1) and/or 6 (R2) aided their tolerance in normal cells. Likewise, the toxicity profile of these compounds in human fibroblasts was supported by the LDH release assay *in vitro* ($p \leq 0.05$). Most of these compounds were active inhibitors of cancer cell proliferation and topo IIα enzyme along with strong

antioxidant capacities. The non-toxic presence of these compounds in human fibroblast *in vitro* and their robust action against the tumor cells certainly enhances and merits their candidacy as potential anti-cancer agents.

Table 4. In vitro toxicity assessment of 3,5-bis(arylmethylene)-1-(*N*-arylmaleamoyl)-4-piperidones (**4A-C, 6A-C, 9Aa-i**, **9Ba-i** and **9Ca-i**) using MTS cell viability and LDH release cytotoxicity assay in WI-38 cells (human fibroblasts).

Compound	Cell Viability	Cytotoxicity	Compound	Cell Viability	Cytotoxicity
4A	81.7±2.8^{def}	14.6±1.2^{efghi}	**9Be**	87.9±2.8^{abcdef}	13.2±0.6^{ghij}
6A	80.5±4.7^{ef}	18.5±1.2^{bcdefg}	**9Bf**	81.6±4.3^{abcdef}	16.1±3.9^{defgh}
9Aa	89.2±3.6^{abcdef}	17.6±0.8^{cdefg}	**9Bg**	87.2±7.1^{abcdef}	14.6±1.7^{efghi}
9Ab	88.2±2.1^{abcdef}	13.2±1.3^{fghij}	**9Bh**	84.1±3.5^{abcdef}	20.7±2.8^{bcde}
9Ac	82.9±4.2^{bcdef}	18.4±0.6^{bcdefg}	**9Bi**	81.4±3.1^{def}	19.7±2.1^{bcdef}
9Ad	90.3±1.5^{abcde}	5.3±0.2^{k}	**4C**	87.2±2.6^{abcdef}	16.3±1.6^{defgh}
9Ae	89.2±1.4^{abcdef}	17.6±0.9^{bcdefg}	**6C**	84.1±3.7^{abcdef}	17.2±2.0^{cdefg}
9Af	80.8±5.3^{ef}	22.9±1.5^{bcd}	**9Ca**	86.8±1.9^{abcdef}	23.1±6.3^{bc}
9Ag	93.1±5.8^{abcd}	13.5±0.7 ^{fghi}	**9Cb**	82.5±1.5^{cdef}	21.7±1.6^{bcd}
9Ah	90.8±3.5^{abcde}	15.8±3.6^{efghi}	**9Cc**	86.1±3.7^{abcdef}	20.4±3.7^{bcde}
9Ai	87.3±2.6^{abcdef}	14.5±1.4^{efghi}	**9Cd**	93.8±1.8^{abc}	18.4±0.5^{bcdefg}
4B	78.8±6.2^{f}	31.3±2.8^{a}	**9Ce**	87.1±2.6^{abcdef}	23.7±3.1^{b}
6B	87.7±1.8^{abcdef}	19.8±2.5^{bcdefg}	**9Cf**	89.6±7.0^{abcdef}	9.3±2.6^{hij}
9Ba	90.8±2.3^{abcde}	9.1±1.1	**9Cg**	86.4±5.6^{abcdef}	17.2±2.3^{cdefg}
9Bb	92.5±5.8^{ab}	17.4±2.7^{bcdefg}	**9Ch**	92.2±4.3^{abcde}	9.5±1.7^{ijk}
9Bc	92.7±1.4^{abcde}	19.3±1.6^{bcdefg}	**9Ci**	87.5±3.5^{abcdef}	16.8±2.4^{defg}
9Bd	82.1±3.0^{cdef}	13.2±0.6^{ghij}	**Curcumin**	95.8±1.4^{a}	7.1±0.6^{jk}

Different values followed by the different superscripted letters (a through k) within column are significantly different; Tukey's multiple means comparison test, $p \leq 0.05$). The compounds were assayed at 100 μM concentration.

2.2.5. In-vivo neurotoxicity studies

Twenty nine compounds (**4C, 9Aa-g, 9Ai, 9Ba-i, 9Cb, 9cd** and **11a-i**) were evaluated for murine toxicity *in vivo* following a literature procedure [42]. All of these compounds were injected intraperitoneally into mice at doses of 30, 100 and 300 mg/kg. The animals were then observed for 0.5 (4, 8 and 4 mice respectively for 30, 100 and 300 mg/kg experiments) and 4 h (2, 4 and 2 mice respectively for 30, 100 and 300 mg/kg experiments) post administration of the compounds. The injected compounds were found to be well-tolerated. Following compounds did not show any signs of toxicity in the experiments: **9Ae**, **9Ag**, **9Bd**, **9Bf**, **9Bg**, **9Bi**, **9Cb**, **9Cd**, **11a**, **11c**, **11g** and **11h**. Death of one animal (out of two) was observed in the case of intermediate **11e** at 300 mg/kg 4 h

post administration. Table 5 summarizes only those cases where some neurological deficit was recorded at a particular dose either during 0.5 h or 4 h observation. These results clearly indicate that the compounds studied here are well-tolerated *in vivo* and are not general biocidal agents.

Table 5: Experimental data on compounds that displayed neurological deficit in the neurotoxicity assay system.

Time			**0.5 h**		**4.0 h**	
Compound	Dose (mg/kg)	Animals tested	Animals showing neurotoxicity	Animals tested	Animals showing neurotoxicity	Mortality
4C	100	8	1	4	0	0
9Aa	100	8	2	4	0	0
	300	4	1	2	1	0
9Ab	100	8	4	4	0	0
9Ac	100	8	1	4	1	0
9Ad	100	8	1	4	1	0
	300	4	3	2	1	0
9Af	100	8	1	4	0	0
	300	4	1	2	1	0
9Ai	300	4	1	2	0	0
9Ba	100	8	2	4	0	0
	300	4	2	2	0	0
9Bb	100	8	3	4	1	0
	300	4	1	2	0	0
9Bc	100	8	1	4	0	0
	300	4	1	2	0	0
9Be	300	4	1	2	0	0
9Bh	30	4	1	2	0	0
	100	8	0	4	1	0
11b	300	4	1	2	0	0
11d	100	8	1	4	0	0
11e	300	4	1	2	1	1 (4 h)
11f	100	8	1	4	0	0
	300	4	1	2	0	0
11i	100	8	1	4	1	0

2.3. Quantitative structure-activity relationship studies

In an attempt to understand how the structural and electronic parameters effect the cytostatic activity of series **9** compounds, a quantitative structure–activity relationship

(QSAR) study was undertaken using certain physicochemical parameters. The extent to which the electrophilicity of the enone systems effected the bioactivity was evaluated by comparing the electronic charge at various β-positions for the three enone systems (calculated using a commercial software) [43] of the test compounds (Charge β_1 and β_2; see Scheme 1 for these locations) with the IC_{50} values against the three cell lines (Table 1). Likewise, the molar refractivity (MR_{mol}) values and the calculated partition coefficient (logP) of series **9** compounds were also obtained using the same commercial software [40] and utilized as a means of assessing the effect of steric properties and lipophilicity, respectively, of the compounds with respect to their bioactivity. Physicochemical parameters of the aromatic substituents [44] such as Taft E_s steric constant for *ortho*-substituents, Hansch π (a measure of the lipophilicity of the substituents), and molar refractivity ($MR_{sub,}$ (a measure of the size of the substituents) were also used for statistical correlation studies. Linear and semilogarithmic correlations were calculated using statistical analysis [45] for the IC_{50} of each tumor cell line and the aforementioned physicochemical parameters. Only the significant correlations obtained are included in Table 6. All significant correlations were obtained in linear as well as semilogarithmic calculations, so in the interest of space and clarity, only the linear correlations are presented.

While several significant correlations were observed for compounds of series **9A** and **9B**, series **9C** compounds did not show any meaningful correlation with the physicochemical properties employed. No significant correlation (P<0.01) was observed between charge β_2 with any of the biological activities for any molecule tested. The correlations obtained for series **9A** compounds are discussed first. A positive significant correlation (P=0.005 or lower) between Taft E_s and antiproliferative activity against Molt4C/8 and CEM cells indicates that decrease in Taft E_s has a decreasing effect (desirable) on the Molt4C/8 and CEM IC_{50} values. A smaller Taft E_s value means larger steric bulk. Thus this correlation predicts that bulky substituent at the *ortho*- position of the substituted aromatic amine moiety will lead to more potent compounds towards Molt4C/8 and CEM cells.

Table 6. Linear Correlation constants between IC_{50} values of compounds of series **9A** and **9B**, and their physicochemical parameters

Series	Independent	Dependent	Correlation coefficient r[a]	P value[b]
Series **9A**	E_s	Molt IC_{50}	0.809	0.005
	E_s	CEM IC_{50}	0.852	0.002
	MR_{sub}	CEM IC_{50}	-0.706	0.023
	MR_{mol}	Molt IC_{50}	-0.565	0.089
	MR_{mol}	CEM IC_{50}	-0.715	0.020
	Hansch π	CEM IC_{50}	-0.555	0.096
	logP	Molt IC_{50}	-0.606	0.063
	logP	CEM IC_{50}	-0.626	0.053
Series **9B**	E_s	CEM IC_{50}	0.711	0.032
	logP	CEM IC_{50}	-0.630	0.069

[a] The magnitude of coefficient r shows the extent (the closer the values to 1, the better) and the nature (sign positive or negative) of the correlation.
[b] The value of P in the range 0.05–0.1 indicates a trend toward significance, while values <0.05 suggest significant correlation.

The same inference is drawn from the negative correlation with significance or trend toward significance between MR_{sub} with CEM IC_{50} values and MR_{mol} with Molt4C/8 and CEM IC_{50} values for series **9A** compounds. This means that as the MR values (MR_{sub} or MR_{mol}) increases, the anticancer IC_{50} value decreases (desirable). Larger MR values signify larger steric bulk. Negative correlations with trend towards significance ($0.1>P>0.05$) were observed between lipophilicity-related parameters Hansch π and logP with Molt4C/8 and CEM IC_{50} values for series **9A** compounds. This indicates that as increased lipophilicity is leading to decreased (desirable) Molt4C/8 and CEM IC_{50} values. Therefore, for future modifications in series **9A** compounds, bulky and more lipophilic substituents at the *ortho*- positions of the substituted aromatic amine moiety should be considered.

For series **9B** compounds, Taft E_s is positively and significantly correlated with CEM IC_{50} values. Thus, to produce more potent series **9B**-based CEM cell growth inhibitor, bulkier substituents (smaller E_s value) at the *ortho*- positions of the substituted aromatic amine moiety are desired. The negative correlation with trend towards significance between logP and CEM IC_{50} values suggests that lipophilicity is desirable for

better anticancer activity. These correlations can be tremendously useful in designing new analogs.

Having obtained the correlation between the cytostatic activities and various physicochemical parameters, we decided to obtain a mathematical equation that describes the relationship between the two using multiple linear regressions for the two series of compounds [42]. For Series **9A** analogs, where CEM IC_{50} correlated with Taft's E_s, Hansch π and MR_{mol}, and Molt IC_{50} correlated with Taft's E_s, logP and MR_{mol}, two equations were obtained:

$$logIC_{50(CEM)} = -0.497 + 0.0873E_s + 0.00219MR_{mol} - 0.0180\pi \quad \text{[R square 77.96\%]}$$

$$logIC_{50(Molt)} = -2.06 + 0.1760E_s + 0.0171MR_{mol} - 0.0896logP \quad \text{[R square 75.91\%]}$$

For Series **9B** compounds, where only CEM IC50 correlated with Taft's E_s and logP, the following linear relationship was obtained:

$$logIC_{50(CEM)} = -0.166 + 0.1127E_s + 0.092logP \quad \text{[R square 59.30\%]}$$

These equations can be used to predict the cytostatic activities of new analogs and future synthesis can be focused on preparing more potent analogs.

3. Conclusions

In conclusion, curcumin-derived three series of novel 3,5-bis(arylmethylene)-1-(*N*-arylmaleamoyl)-4-piperidones inhibited proliferation of human Molt 4/C8 and CEM T-lymphocytes as well as murine L1210 leukemic cells. The enhancement in anticancer potency in comparison with melphalan and curcumin was 93-280 folds. It is apparent from these data that curcumin-derived piperidones are potent cytostatic agents *in vitro* with widespread efficacy in multiple cell lines at low concentrations. Several novel compounds (such as **9Aa, 9Ad** and **9Af**) displayed excellent inhibition of cancer cell proliferation in multiple cancer cell lines including breast cancer, central nervous system, colon, leukemia, melanoma, non-small cell lung, ovarian, prostate and renal cancer. These may effectively serve as leads for further analysis and development of 'Swiss army

knives' for curcumin-inspired cancer research. The multifunctional curcumin-derived compounds also displayed interesting properties as topoisomerase IIα inhibitory activity and antioxidant action. Likewise, the safety profile of these compounds in both *in vitro* and *in vivo* models make them it a safe candidate for further evaluation in animals and subsequently in humans.

4. Experimental section

4.1. Materials and methods

All reagents and solvents were used as supplied by commercial sources without further purification. Anhydrous solvent THF was obtained by distilling from sodium and benzophenone. Oven dried glassware and an atmosphere of nitrogen was used for moisture sensitive reactions. Precoated fluorescent silica gel TLC plates were used to monitor the progress of the reactions. Silica gel 60 (SiliaFlash P60, Silicycle, Quebec City, Canada) was used for flash chromatography. Melting points were measured using a MEL-TEMP II apparatus and are uncorrected. IR spectra were recorded on a Nicolet MAGNA-IR 560 Spectrophotometer. ^{1}H and ^{13}C NMR were recorded on a Bruker AV500 spectrophotometer at 500 and 125 MHz, respectively in DMSO-d_6 as the solvent. Chemical shifts of the ^{1}H NMR spectra are reported in parts per million (ppm) downfield from tetramethylsilane. UV-Vis spectra were recorded on a LKB Biochrom Ultraspec Plus 4054 UV/Visible spectrophotometer. ESI-HRMS were recorded on a microTOF (Bruker Daltonics) spectrometer.

4.2. General synthesis

4.2.1. General procedure for the synthesis of 3,5-bisarylidene-piperidin-4-ones (4A-C)

To a 250 mL round bottom oven dried flask, was added, 4-piperidone hydrate hydrochloride (0.10 mol), appropriate aromatic aldehyde (0.20 mol), acetic acid (150 ml). The reaction mixture was sealed and HCl (g) was passed through the reaction flask for 30 minutes while the reaction was stirred. During this time, the clear mixture yielded thick yellow or orange precipitates. After the 30 minute period, the HCl gas was turned off and the reaction was left to stir for 24 hours. The precipitate was then filtered using suction filtration. The products as acid salts thus obtained were quite pure and were used for

subsequent reactions without further purification.

4.2.1.1. 3, 5-Bisbenzylidene-piperidin-4-one hydrochloride (4A)

Yellow power, yield 71%, m.p. 243-246 °C (lit. [46] m.p. 242-243). NMR spectral data was found to be identical to those reported in the literature.[46]

4.2.1.2. 3, 5-Bis-4-nitrobenzylidene-piperidin-4-one hydrochloride (4B)

Orange powder, yield 65%, m.p. 286-289 °C (lit. [36] m.p. 242-243 free base). NMR spectral data was found to be identical to those reported in the literature.[36]

4.2.1.3. 3,5-Bis-[1-(4-carboethoxy-phenyl)-meth-(E)-ylidenel-piperidin-4-one acetic acid salt (4C)

Yellow powder, yield 60%, m.p. 225-221 °C. ^{1}H NMR (500 MHz, DMSO-d_6): 1.35 (t, *J* = 7.0 *Hz*, 6 H), 1.92 (s, 3H), 4.36 (q, *J* = 7.0 *Hz*, 4H), 4.50 (s, 4H), 7.68 (d, *J* = 8.0 *Hz*, 4H), 7.92 (s, 2H), 8.08 (d, *J* = 8.0 *Hz*, 4H), 10.03 (s, 2H). ^{13}C NMR (125 MHz, DMSO-d_6): δ 14.1, 21.0, 43.6, 61.0, 129.4, 129.7, 130.5, 130.6, 137.9, 138.1, 165.1, 171.9, 182.2 (23/25). UV (λ_{max}, EtOH): 217, 244, 315 nm. ESI-HRMS (amu): calcd. $C_{25}H_{25}NO_5$: 420.1811 [M+H]; found: 420.1824.

4.2.2. *N*-Acryloyl-3,5-bis-[1-(4-carboethoxy-phenyl)-meth-(*E*)-ylidenel-piperidin-4-one (6C)

Compound **4C** (0.006 mol) and triethylamine (0.014 mol) were dissolved in dry DCM (50 mL) and cooled to 0 ^{o}C using an ice bath. Under anhydrous conditions, acryloyl chloride (0.007 mol) in dry DCM (30 mL) was added dropwise over a 10 minute period. The mixture was stirred for 24 hours at room temperature. The solvents were then evaporated under vacuum. Water (30 mL) was added to the residue and the product was triturated and filtered. Under suction filtration, the solid product was washed with 10% HCl, and then distilled water, and then a saturated potassium carbonate solution. The solid product was washed once again with distilled water. The product was digested in methanol to remove unwanted side products and unreacted starting materials. It was then filtered and washed with cold methanol. The final product was filtered by suction filtration and dried. Characterization data: Yellow powder, yield 62%, m.p. 120-123 °C. ^{1}H NMR (500 MHz, DMSO-d_6): 1.35 (t, *J* = 7.0 *Hz*, 6 H), 4.35 (q, *J* = 7.0 *Hz*, 4H), 4.92-4.96 (m, 4H), 5.58 (d, *J* = 10.5 *Hz*, 1H), 6.00 (d, *J* = 17.0 *Hz*, 1H), 6.55 (dd, *J* = 17.0 &

11.0 *Hz*, 1H), 7.65-7.74 (m, 6H), 8.06 (d, *J* = 8.0 *Hz*, 4H). ^{13}C NMR (125 MHz, DMSO-d_6): δ 14.6, 43.6, 61.5, 127.8, 128.9, 129.9, 130.8, 131.1, 134.7, 135.5, 165.4, 165.7, 168.8, 186.4 (23/25). ESI-HRMS (amu): calcd. $C_{28}H_{27}NO_6$: 496.1736 [M+Na]; found: 496.1735.

4.2.3. General procedure to synthesize aryl maleamic acids (11a-i)

Maleic anhydride (0.004 mol) and the appropriate aryl amine (0.004 mol) were dissolved in dichloromethane (100 mL) and were stirred for a time period that ranged between 30 min to 48 h depending on the aryl amine used. Heat was also applied for certain aryl amides to speed up the reaction. TLC plates were used to monitor the progress of the reactions (5% methanol:dichloromethane). The solvents were removed by vacuum, the precipitates were then washed with dichloromethane, filtered under suction and dried. The aryl maleamic acids were obtained as powders and were very pure as was evident by their melting points and their NMR spectra.

Deviations from procedure: Compounds **11d** and **11f** had to be stirred for 48 h and heat had to be applied for one hour. The reactions still did not go all the way to completion so the solvents were removed by suction filtration rather than vacuum. Compound **11i** had to be stirred for 12 h, compounds **11g** and **11h** needed stirring for 4 h and reactions leading to compounds **11a**, **11b**, **11c** and **11e** were complete within 30 min.

4.2.3.1. (2-Flurophenyl)-maleamic acid (11a)

Yellow powder, 87%, m.p. 153-154°C (lit. [47] m.p. 163 ^{o}C). Its NMR spectral data was found to be identical to those reported in the literature [47].

4.2.3.2. (2-Chlorophenyl)-maleamic acid (11b)

Yellow powder, yield 84%, m.p. 129-132 °C (lit. [48] m.p. 134-136 ^{o}C). Its NMR spectral data was found to be identical to those reported in the literature [48].

4.2.3.3. (2-Methylphenyl)-maleamic acid (11c)

White powder, yield 58%, m.p. 116-120 °C (lit. [49] m.p. 104-105 ^{o}C). Its NMR spectral data was found to be identical to those reported in the literature [49].

4.2.3.4. (2-Methyoxyphenyl)-maleamic acid (11d)

Green powder, yield 99%, m.p. 144-146 °C (lit. [49] m.p. 134-136 ^{o}C). Its NMR spectral data was found to be identical to those reported in the literature [49].

4.2.3.5. (2-Nitrophenyl)-maleamic acid (11e)

Yellow powder, yield 31%, m.p. 132-133 °C (lit. [50] m.p. 138-140 ^{o}C). ^{1}H NMR (300 MHz, DMSO-d_6): δ 6.40 (d, 1H, J=12.0Hz), 6.50 (d, 1H, J=11.9Hz), 7.38-7.44 (m, 1H), 7.68-7.76 (m, 2H), 7.98 (d, 1H, J=8.2Hz), 10.60 (s, 1H). UV (λ_{max}, EtOH): 217, 384 nm. IR (ν, KBr): 501, 695, 738, 912, 1214, 1279, 1353, 1520, 1587, 1712, 2599, 2950, 3016 cm^{-1}.

4.2.3.6. (2,6-Dichlorophenyl)-maleamic acid (11f)

Yellow powder, 25%, m.p. 158-159 °C. ^{1}H NMR (300 MHz, DMSO-d_6): δ 6.44 (d, 2H), 6.60 (d, 2H), 7.38 (t, 1H, J=8.4Hz), 7.57 (d, 2H, J=8.2Hz), 10.39 (s, 1H). UV (λ_{max}, EtOH): 216 nm. IR (ν, KBr): 540, 790, 875, 1300, 1450, 1490, 1550, 1620, 1700, 2998, 3008, 3200 cm^{-1}.

4.2.3.7. (2,6-Dimethylphenyl)maleamic acid (11g)

White powder, yield 87%, m.p. 173-175 °C. (lit. [51] m.p. 170-173 ^{o}C). Its NMR spectral data was found to be identical to those reported in the literature [51].

4.2.3.8. (2,4,6-Trimethylphenyl)-maleamic acid (11h)

Yellow powder (76.4%, 0.71g); R_f 0.40 (5% CH_3OH: CH_2Cl_2); m.p. 104-105 °C. (lit. [52] m.p. 99-100 ^{o}C). Its NMR spectral data was found to be identical to those reported in the literature [52].

4.2.3.9. (2-Ethyl-6-methylphenyl)-maleamic acid (11i)

Grey powder, yield 66%, m.p. 150-152 °C. ^{1}H NMR (300 MHz, DMSO-d_6): δ 1.09 (t, 3H, J=7.5Hz), 2.16 (s, 3H), 2.60 (qt, 2H, J=7.6Hz), 6.32 (d, 1H, J=12.3Hz), 6.60 (d, 1H, J=12.3Hz), 7.10-7.15 (m, 3H), 10.00 (s, 1H). UV (λ_{max}, EtOH): 241 nm. IR (ν, KBr): 622, 862, 907, 980, 1249, 1309, 1520, 1632, 1660, 2964, 3254 cm^{-1}.

4.2.4. General procedure for the synthesis of 4-(3,5-bisarylmethylene-4-oxo-piperidin-1-yl)-4-oxo-but-2-enoic acid arylamides (9Aa-i, 9Ba-i and 9Ca-i)

The appropriate aryl maleamic acid (0.006 mol) and triethylamine (0.006 mol) were dissolved in dry THF (50 mL) and cooled to 0 ^{o}C using an ice bath. Under anhydrous conditions, ethyl chloroformate (0.006 mol) in dry THF (40 mL) was added

dropwise over a 10 minute period. The mixture was stirred for 24 hours at room temperature, cooled to 0 ^{o}C and appropriate 3,5-bisarylmethylene-piperidin-4-one (0.0042 mol) was added. Subsequently triethylamine (0.006 mol) in dry THF (40 mL) was added dropwise over 10 minutes. The reaction was then stirred for 24 hours during which time the temperature slowly rose to room temperature. The solvents were then evaporated under vacuum. Water (30 mL) was added to the residue and the product was triturated and filtered. Under suction filtration, the solid product was washed with 10% HCl, and then distilled water, and then a saturated potassium carbonate solution. The solid product was washed once again with distilled water. The product was digested in methanol to remove unwanted side products and unreacted starting materials. It was then filtered and washed with cold methanol. The final product was filtered by suction filtration and dried. The reactions were monitored by TLC (5% methanol: dichloromethane).

Deviations from procedure: Compound **9Ah** was completely soluble in methanol so the unwanted side products had to be removed by column chromatography (0-3% MeOH: Dichloromethane). The final product was obtained after vacuum evaporation.

4.2.4.1. (2*Z*)-4-(3*E*,5*E*)-(3,5-Bisbenzylidene-4-oxo-piperidine-4-oxo-piperidin-1-yl)-4-oxo-but-2-enoic acid (2-flurophenyl)amide (9Aa):

Yellow powder, yield 64%, m.p. 171-173 °C. ^{1}H NMR (500 MHz, DMSO-d_6): δ 4.78 & 4.93 (s, 2H each), 6.25 & 6.49 (d, J = 11.5 Hz, 1H each), 7.18-7.62 (m, 14H), 7.77 (s, 1H), 7.95-7.98 (m, 1H), 9.89 (s, 1H). ^{13}C NMR (125 MHz, DMSO-d_6): δ 41.2, 46.7, 115.3 (d, J = 20 Hz), 124.3, 125.3 (d, J = 7 Hz), 125.6, 125.7, 125.8, 128.7, 128.8, 129.3, 129.5, 130.0, 130.5, 132.1, 134.3 (d, J = 20 Hz), 134.9, 135.4, 136.3, 153.0 (d, J = 244 Hz), 162.1, 166.3, 185.4. UV (λ_{max}, EtOH): 326 nm. IR (ν, KBr): 501, 518, 561, 599, 666, 698, 753, 807, 886, 985, 1105, 1180, 1242, 1276, 1487, 1538, 1621, 1636, 1685, 2824, 3051, 3320 cm^{-1}. ESI-HRMS (amu): calcd. $C_{29}H_{23}FN_2O_3$: 489.1590 [M+Na]; found: 489.1582.

4.2.4.2. (2*Z*)-4-(3*E*,5*E*)-(3,5-Bisbenzylidene-4-oxo-piperidine-4-oxo-piperidin-1-yl)-4-oxo-but-2-enoic acid (2-chlorophenyl)amide (9Ab)

Yellow powder, yield 54%, m.p. 160-162 °C. ^{1}H NMR (500 MHz, DMSO-d_6): δ 4.78 & 4.91 (s, 2H each), 6.30 & 6.52 (d, *J* = 12.0 Hz), 7.22 (t, *J* = 7.5 Hz, 1H), 7.34-7.63 (m, 13H), 7.76 (s, 2H), 9.66 (brs, 1H). ^{13}C NMR (125 MHz, DMSO-d_6): δ 41.6, 46.8, 125.5, 125.6, 125.9, 126.4, 127.3 128.7, 128.8, 129.3, 129.4, 129.5, 130.1, 130.5, 132.0, 134.3, 134.3, 134.4, 135.1, 135.5, 136.2, 162.1, 166.3, 185.4. UV (λ_{max}, EtOH): 325, 327 nm. IR (ν, KBr): 436, 517, 699, 759, 803, 884, 945, 1039, 1179, 1240, 1274, 1441, 1529, 1622, 1637, 1686, 2825, 3332 cm^{-1}. ESI-HRMS (amu): calcd. $C_{29}H_{23}ClN_2O_3$: 505.1295 [M+Na]; found: 505.1285.

4.2.4.3. (2*Z*)-4-(3*E*,5*E*)-(3,5-Bisbenzylidene-4-oxo-piperidine-4-oxo-piperidin-1-yl)-4-oxo-but-2-enoic acid (2-methylphenyl)amide (9Ac)

Yellow powder, yield 39%, m.p. 170-171 °C. ^{1}H NMR (500 MHz, DMSO-d_6): δ 2.15 (s, 3H), 4.80 & 4.90 (s, 2H each), 6.19 & 6.47 (d, *J* = 11.5 Hz, 1H each), 7.11 (t, *J* = 7.5 Hz, 1H), 7.17-7.24 (m, 2H), 7.41-7.60 (m, 11H), 7.63 & 7.75 (s, 1H each), 9.44 (brs, 1H). ^{13}C NMR (125 MHz, DMSO-d_6): δ 18.3, 42.1, 47.4, 125.0, 125.8, 126.4, 126.5, 127.3, 129.3, 129.9, 130.0, 130.7, 130.8, 131.0, 131.9, 132.6, 132.9, 134.7, 134.8, 134.9, 136.0, 136.2, 136.7, 162.3, 167.0, 185.9. UV (λ_{max},EtOH): 326 nm. IR (ν, KBr): 496, 517, 605, 697, 758, 803, 882, 946, 984, 1178, 1242, 1275, 1443, 1455, 1532, 1586, 1620, 1636, 1684, 1733, 2334, 2362, 2835, 3054, 3375 cm^{-1}. ESI-HRMS (amu): calcd. $C_{30}H_{26}N_2O_3$: 485.1841 [M+Na]; found: 485.1835.

4.2.4.4. (2*Z*)-4-(3*E*,5*E*)-(3,5-Bisbenzylidene-4-oxo-piperidine-4-oxo-piperidin-1-yl)-4-oxo-but-2-enoic acid (2-methoxyphenyl)amide (9Ad)

Yellow powder, yield 55%, m.p. 179-181 °C. ^{1}H NMR (500 MHz, DMSO-d_6): δ 3.83 (s, 3H), 4.78 & 4.92 (s, 2H each), 6.36 & 6.42 (d, *J* = 11.5 Hz, 1H each), 6.94 (t, *J* = 7.5 Hz, 1H), 7.06 (d, *J* = 8.0 Hz, 1H), 7.11 (t, *J* = 7.5 Hz, 1H), 7.32 (brs, 2H), 7.41 (brs, 3H), 7.46-7.61 (m, 6H), 7.77 (s, 1H), 7.99 (d, *J* = 7.5 Hz, 1H), 9.31 (s, 1H). ^{13}C NMR (125 MHz, DMSO-d_6): δ 42.1, 47.3, 56.1, 111.6, 120.7, 122.1, 125.1, 127.0, 127.4, 129.2, 129.3, 129.8, 130.0, 130.6, 131.0, 132.6, 132.9, 134.5, 134.8, 134.9, 136.0, 136.7, 149.9, 162.4, 167.1, 185.9. UV (λ_{max}, EtOH): 204, 207, 249, 323 nm. IR (ν, KBr): 491, 522, 541, 630, 698, 755, 771, 809, 940, 991, 1021, 1045, 1114, 1177, 1249, 1284, 1331, 1524, 1681, 3397 cm^{-1}. ESI-HRMS (amu): calcd. $C_{30}H_{26}N_2O_4$: 501.1790 [M+Na]; found: 501.1797.

4.2.4.5. (2*Z*)-4-(3*E*,5*E*)-(3,5-Bisbenzylidene-4-oxo-piperidine-4-oxo-piperidin-1-yl)-4-oxo-but-2-enoic acid (2-nitrophenyl)amide (9Ae)

Yellow powder, yield 66%, m.p. 186-188 °C. ^{1}H NMR (500 MHz, DMSO-d_6): δ 4.76 & 4.89 (s, 2H each), 6.19 & 6.56 (d, *J* = 12.0 Hz, 1H each), 7.40-7.60 (m, 11H), 7.63 (s, 1H), 7.72-7.78 (m, 3H), 8.01 (d, *J* = 8.5 Hz, 1H), 10.42 (brs, 1H). ^{13}C NMR (125 MHz, DMSO-d_6): δ 41.6, 46.7, 125.0, 125.1, 125.3, 125.5, 128.7, 128.8, 129.4, 129.5, 130.2, 130.5, 130.8, 132.0, 134.1, 134.2, 134.3, 135.7, 135.9, 142.0, 162.0, 166.0, 185.4. UV (λ_{max}, EtOH): λmax: 204, 207, 327, 329 nm. IR (ν, KBr): 518, 599, 668, 694, 744, 802, 940, 983, 1174, 1280, 1341, 1436, 1498, 1652, 1699, 1772, 2338, 2362, 3374, 3853 cm^{-1}. ESI-HRMS (amu): calcd. $C_{29}H_{23}N_3O_5$: 516.1535 [M+Na]; found: 516.1524.

4.2.4.6. (2*Z*)-4-(3*E*,5*E*)-3,5-Bisbenzylidene-4-oxo-piperidine-4-oxo-piperidin-1-yl)-4-oxo-but-2-enoic acid (2,6-dichlorophenyl)amide (9Af)

Yellow powder, yield 47%, m.p. 197-200 °C. ^{1}H NMR (500 MHz, DMSO-d_6): δ 4.78 & 4.86 (s, 2H each), 6.21 & 6.55 (d, *J* = 12.0 Hz, 1H each), 7.37 (t, *J* = 8.5 Hz, 1H), 7.47-7.57 (m, 12H), 7.64 & 7.72 (s, 1H each), 10.13 (brs, 1H). ^{13}C NMR (125 MHz, DMSO-d_6): δ 41.8, 47.3, 124.6, 129.0, 129.1, 129.3, 129.8, 130.0, 130.8, 130.9, 132.5, 132.6, 132.9, 134.0, 134.9, 136.3, 136.7, 162.2, 166.7, 185.9. UV (λ_{max}, EtOH) 204, 227, 328 nm. IR (ν, KBr): 516, 537, 667, 695, 779, 943, 978, 1133, 1171, 1242, 1277, 1435, 1471, 1490, 1531, 1571, 1617, 1673, 2362, 3525 cm^{-1}. ESI-HRMS (amu): calcd. $C_{29}H_{22}Cl_2N_2O_3$: 539.0905 [M+Na]; found: 539.0887.

4.2.4.7. (2*Z*)-4-(3*E*,5*E*)-(3,5-Bisbenzylidene-4-oxo-piperidine-4-oxo-piperidin-1-yl)-4-oxo-but-2-enoic acid (2,6-dimethylphenyl)amide (9Ag)

Yellow powder, yield 83%, m.p. 204-206 °C. ^{1}H NMR (500 MHz, DMSO-d_6): δ 2.09 (s, 6H), 4.80 & 4.97 (s, 2H each), 6.19 & 6.49 (d, *J* = 11.5 Hz, 1H each), 7.06-7.08 (m, 3H), 7.46-7.57 (m, 10H), 7.64 & 7.72 (s, 1H each), 9.48 (brs, 1H). ^{13}C NMR (125 MHz, DMSO-d_6): δ 18.0, 41.4, 46.9, 125.3, 126.5, 127.6, 128.6, 128.8, 129.4, 130.2, 130.4, 132.0, 132.2, 134.3, 134.4, 134.5, 134.9, 135.6, 136.1, 161.5, 166.4, 185.3. UV (λ_{max}, EtOH) 204, 328 nm. IR (ν, KBr): 516, 526, 695, 770, 943, 977, 1170, 1241, 1442, 1469, 1527, 1617, 1663, 1733, 2339, 2362, 3235 cm^{-1}. ESI-HRMS (amu): calcd. $C_{31}H_{28}N_2O_3$: 499.1998 [M+Na]; found: 499.1989.

4.2.4.8. (2*Z*)-4-(3*E*,5*E*)-(3,5-Bisbenzylidene-4-oxo-piperidine-4-oxo-piperidin-1-yl)-4-oxo-but-2-enoic acid (2,4,6-trimethylphenyl)amide (9Ah)

Yellow powder, yield 36%, m.p. 194-196 °C. ^{1}H NMR (500 MHz, DMSO-d_6): δ 2.04 (s, 6H), 2.23 (s, 3H), 4.79 & 4.86 (s, 2H each), 6.17 & 6.46 (d, *J* = 11.5 Hz, 1H each), 6.88 (s, 2H), 7.45-7.57 (m, 10H), 7.64 & 7.72 (s, 1H each), 9.37 (brs, 1H). ^{13}C NMR (125 MHz, DMSO-d_6): δ 18.4, 21.0, 41.9, 47.4, 125.8, 128.2, 128.7, 129.0, 129.3, 130.0, 130.7, 130.9, 132.3, 132.6, 132.7, 134.7, 134.8, 134.9, 135.1, 136.0, 136.6, 162.1, 167.0, 185.8. UV (λ_{max}, EtOH): 219, 328 nm. IR (ν, KBr): 516, 671, 749, 808, 984, 1174, 1237, 1277, 1436, 1616, 1675, 1683,1733, 2915, 3675, 3780, 3853 cm^{-1}. ESI-HRMS (amu): calcd. $C_{32}H_{30}N_2O_3$: 513.2154 [M+Na]; found: 513.2138.

4.2.4.9. (2*Z*)-4-(3*E*,5*E*)-(3,5-Bisbenzylidene-4-oxo-piperidine-4-oxo-piperidin-1-yl)-4-oxo-but-2-enoic acid (2-ethyl-6-methylphenyl)amide (9Ai)

Yellow powder, yield 28%, m.p. 181-184 °C. ^{1}H NMR (500 MHz, DMSO-d_6): δ 1.04 (t, *J* = 7.5 Hz, 3H), 2.08 (s, 3H), 2.45 (q, *J* = 7.5 Hz, 2H), 4.79 & 4.86 (s, 2H each), 6.20 & 6.49 (d, *J* = 11.5 Hz, 1H each) 7.09-7.57 (m, 13H), 7.64 & 7.72 (s, 1H each), 9.47 (brs, 1H). ^{13}C NMR (125 MHz, DMSO-d_6): δ 14.4, 18.0, 24.2, 41.4, 46.9, 125.2, 125.9, 126.7, 126.9, 127.0, 127.4, 127.7, 128.2, 128.5, 128.7, 129.2, 130.2, 130.4, 132.0, 133.8, 134.3, 134.5, 135.5, 136.1, 140.7, 162.0, 166.5, 185.3. UV (λ_{max}, EtOH): 328 nm. IR (ν, KBr): 516, 687, 760, 806, 938, 986, 1174, 1191, 1253, 1277, 1443, 1528, 1581, 1626, 1673, 2969, 3222 cm^{-1}. ESI-HRMS (amu): calcd. $C_{32}H_{30}N_2O_3$: 513.2154 [M+Na]; found: 513.2135.

4.2.4.10. (2*Z*)-4-(3*E*,5*E*)-(3,5-Bis-4-nitrobenzylidene-4-oxo-piperidin-1-yl)-4-oxo-but-2-enoic acid (2-flurophenyl)amide (9Ba)

Yellow powder, yield 47%, m.p. 192-194 °C. ^{1}H NMR (500 MHz, DMSO-d_6): δ 4.78 & 4.95 (s, 2H each), 6.21 & 6.47 (d, *J* = 11.5 Hz, 1H each), 7.19-7.21 (m, 2H), 7.26-7.31 (m, 1H), 7.53 (d, *J* = 8.5 Hz, 1H), 7.60 & 7.84 (s, 1H each), 7.87 (d, *J* = 8.5 Hz, 1H), 7.93-7.96 (m, 1H), 8.22 & 8.34 (d, *J* = 8.5 Hz, 2H each), 9.82 (brs, 1H). ^{13}C NMR (125 MHz, DMSO-d_6): δ 42.2, 47.0, 115.9 (d, *J* = 20 Hz), 123.8, 124.1, 124.3, 124.9, 125.7 (d, *J* = 6 Hz), 126.2, 126.3, 131.5, 132.0, 133.6, 134.8, 135.4, 135.8, 141.2, 141.3, 147.6, 147.8, 153.6 (d, *J* = 245 Hz), 162.5, 167.0, 185.6. UV (λ_{max}, EtOH): 242, 331 nm. IR (ν, KBr): 701, 756, 768, 854, 867, 982, 1107, 1174, 1243, 1255, 1282, 1345, 1457, 1511,

1537, 1596, 1621, 1645, 1686, 2362, 3310 cm^{-1}. ESI-HRMS (amu): calcd. $C_{29}H_{21}FN_4O_7$: 579.1292 [M+Na]; found: 579.1264.

4.2.4.11. (2*Z*)-4-(3*E*,5*E*)-(3,5-Bis-4-nitrobenzylidene-4-oxo-piperidin-1-yl)-4-oxo-but-2-enoic acid (2-chlorophenyl)amide (9Bb)

Yellow powder, yield 67%, m.p. 207-210 °C. ^{1}H NMR (300 MHz, DMSO-d_6): δ 4.78 & 4.93 (s, 2H each), 6.25 & 6.51 (d, *J* = 11.5 Hz, 1H each), 7.22 (t, *J* = 7.5 Hz, 1H), 7.36 (t, *J* = 7.5 Hz, 1H), 7.51 (d, *J* = 8.0 Hz, 1H), 7.62 (d, *J* = 8.5 Hz, 2H), 7.66 (s, 1H), 7.75 (t, *J* = 8.5 Hz, 1H), 7.82 (s, 1H), 7.86, 8.26 & 8.33 (d, *J* = 8.5 Hz, 2H each), 9.61 (brs, 1H). ^{13}C NMR (125 MHz, DMSO-d_6): δ 42.2, 47.1, 124.1, 124.2, 124.3, 125.9, 126.2, 126.9, 127.9, 130.0, 131.5, 131.9, 132.0, 133.7, 134.7, 134.8, 135.4, 135.6, 135.8, 141.3, 147.7, 147.8, 162.5, 167.0, 185.6. UV (λ_{max}, EtOH): 218, 329 nm. IR (ν, KBr): 618, 755, 767, 853, 983, 1107, 1174, 1345, 1510, 1524, 1593, 1620, 1685, 3365 cm^{-1}. ESI-HRMS (amu): calcd. $C_{29}H_{21}ClN_4O_7$: 595.0996 [M+Na]; found: 595.1014.

4.2.4.12. (2*Z*)-4-(3*E*,5*E*)-(3,5-Bis-4-nitrobenzylidene-4-oxo-piperidin-1-yl)-4-oxo-but-2-enoic acid (2-methylphenyl)amide (9Bc)

Yellow powder, yield 74%, m.p. 195-198 °C. ^{1}H NMR (500 MHz, DMSO-d_6): δ 2.13 (s, 3H), 4.80 & 4.92 (s, 2H each), 6.16 & 6.46 (d, *J* = 11.5 Hz, 1H each), 7.12 (t, *J* = 7.5 Hz, 1H), 7.17-7.23 (m, 2H), 7.42 (d, *J* = 8.0 Hz, 1H), 7.64-7.68 (m, 3H), 7.81 (s, 1H), 7.86, 8.27 & 8.33 (d, *J* = 8.5 Hz, 2H each), 9.61 (brs, 1H). ^{13}C NMR (125 MHz, DMSO-d_6): δ 18.3, 42.1, 47.2, 124.2, 124.3, 124.8, 125.8, 126.4, 130.8, 131.6, 131.7, 132.0, 133.7, 134.7, 135.4, 135.8, 136.2, 141.3, 147.7, 147.8, 162.3, 167.2, 185.6. UV (λ_{max}, EtOH): 207, 209, 220 nm. IR (ν, KBr): 516, 592, 701, 755, 854, 866, 982, 1108, 1129, 1172, 1255, 1282, 1345, 1454, 1509, 1525, 1589, 1620, 1644, 1683, 3411 cm^{-1}. ESI-HRMS (amu): calcd. $C_{30}H_{24}N_4O_7$: 575.1543 [M+Na]; found: 575.1512.

4.2.4.13. (2*Z*)-4-(3*E*,5*E*)-(3,5-Bis-4-nitrobenzylidene-4-oxo-piperidin-1-yl)-4-oxo-but-2-enoic acid (2-methoxyphenyl)amide (9Bd)

Yellow powder, yield 50%, m.p. 220-224 °C. ^{1}H NMR (500 MHz, DMSO-d_6): δ 3.84 (s, 3H), 4.77 & 4.94 (s, 2H each), 6.32 & 6.40 (d, *J* = 12.0 Hz, 1H each), 6.94 (t, *J* = 7.5 Hz, 1H), 7.05 (d, *J* = 8.0 Hz, 1H), 7.12 (t, *J* = 7.5 Hz, 1H), 7.51 (d, *J* = 8.5 Hz, 2H), 7.60 & 7.84 (s, 1H each), 7.89 (d, *J* = 8.5 Hz, 2H), 7.97 (d, *J* = 8.0 Hz, 1H), 8.20 & 8.35 (d, *J* = 8.5 Hz, 2H each), 9.25 (brs, 1H). ^{13}C NMR (125 MHz, DMSO-d_6): δ 42.1, 47.1,

56.1, 111.6, 120.7, 121.9, 124.1, 124.3, 125.1, 127.0, 127.3, 131.5, 132.0, 133.6, 134.4, 134.7, 135.5, 135.8, 141.2, 141.4, 147.6, 147.8, 149.8, 162.3, 167.3, 185.7. UV (λ_{max}, EtOH): 329 nm. IR (ν, KBr): 770, 804, 852, 859, 926, 982, 1018, 1046, 1104, 1169, 1252, 1278, 1341, 1355, 1458, 1514, 1596, 1624, 1679, 3388 cm^{-1}. ESI-HRMS (amu): calcd. $C_{30}H_{24}N_4O_8$: 591.1492 [M+Na]; found: 591.1482.

4.2.4.14. (2*Z*)-4-(3*E*,5*E*)-(3,5-Bis-4-nitrobenzylidene-4-oxo-piperidin-1-yl)-4-oxo-but-2-enoic acid (2-nitrophenyl)amide (9Be)

Yellow powder, yield 69%, m.p. 214-216 °C. ^{1}H NMR (300 MHz, DMSO-d_6): δ 4.76 & 4.91 (s, 2H each), 6.15 & 6.55 (d, *J* = 12.0 Hz, 1H each), 7.42 (t, *J* = 7.5 Hz, 1H), 7.65-7.87 (m, 8H), 8.00 (d, *J* = 8.0 Hz, 1H), 8.27 & 8.32 (d, *J* = 8.5 Hz, 2H each), 10.36 (brs, 1H). ^{13}C NMR (125 MHz, DMSO-d_6): δ 42.1, 47.1, 124.1, 124.3, 125.5, 125.7, 125.8, 126.1, 131.2, 131.7, 132.0, 134.0, 134.6, 134.8, 135.3, 135.5, 136.3, 141.3, 142.5, 147.7, 147.8, 162.5, 166.7, 185.6. UV (λ_{max}, EtOH): 223, 332 nm. IR (ν, KBr): 745, 805, 853, 993, 1176, 1276, 1342, 1503, 1516, 1584, 1626, 1647, 1687, 3344 cm^{-1}. ESI-HRMS (amu): calcd. $C_{29}H_{21}N_5O_9$: 606.1237 [M+Na]; found: 606.1226.

4.2.4.15. (2*Z*)-4-(3*E*,5*E*)-(3,5-Bis-4-nitrobenzylidene-4-oxo-piperidin-1-yl)-4-oxo-but-2-enoic acid (2,6-dichlorophenyl)amide (9Bf)

Yellow powder, yield 58%, m.p. 213-215 °C. ^{1}H NMR (500 MHz, DMSO-d_6): δ 4.78 & 4.88 (s, 2H each), 6.18 & 6.55 (d, *J* = 12.0 Hz, 1H each), 7.36 (t, *J* = 8.0 Hz, 1H), 7.54 (d, *J* = 8.5 Hz, 2H), 7.70 (s, 1H), 7.73 (d, *J* = 8.5 Hz, 2H), 7.78 (s, 1H), 7.83 (d, *J* = 8.5 Hz, 2H), 8.29-8.33 (m, 4H), 10.10 (brs, 1H). ^{13}C NMR (125 MHz, DMSO-d_6): δ 41.9, 47.2, 124.1, 124.2, 124.9, 129.0, 129.8, 131.7, 132.0, 132.8, 133.9, 134.0, 134.6, 135.2, 135.5, 136.1, 141.2, 141.4, 147.7, 147.8, 162.1, 166.8, 185.6. UV (λ_{max}, EtOH): 210, 243, 333 nm. IR (ν, KBr): 755, 783, 806, 855, 935, 993, 1191, 1252, 1275, 1345, 1437, 1452, 1518, 1597, 1625 cm^{-1}. ESI-HRMS (amu): calcd. $C_{29}H_{20}Cl_2N_4O_7$: 607.0787 [M+H]; found: 607.0783.

4.2.4.16. (2*Z*)-4-(3*E*,5*E*)-(3,5-Bis-4-nitrobenzylidene-4-oxo-piperidin-1-yl)-4-oxo-but-2-enoic acid (2,6-dimethylphenyl)amide (9Bg)

Yellow powder, yield 54%, m.p. 205-208 °C. ^{1}H NMR (500 MHz, DMSO-d_6): δ 2.05 (s, 6H), 4.81 & 4.89 (s, 2H each), 6.16 & 6.49 (d, *J* = 11.5 Hz, 1H each), 7.05-7.09 (m, 3H), 7.70 (s, 1H), 7.75 (d, *J* = 8.5 Hz, 2H), 7.78 (s, 1H), 7.83 (d, *J* = 8.0 Hz, 2H),

8.31 (d, *J* = 8.0 Hz, 4H), 9.43 (brs, 1H). ^{13}C NMR (125 MHz, DMSO-d_6): δ 18.5, 41.9, 47.3, 124.2, 126.0, 127.0, 128.1, 131.7, 131.9, 133.8, 134.6, 134.8, 134.9, 135.3, 135.4, 135.7, 141.3, 141.4, 147.7, 147.8, 162.0, 167.1, 185.6. UV (λ_{max}, EtOH): 207, 247, 333 nm. IR (ν, KBr): 667, 806, 854, 991, 1174, 1189, 1249, 1276, 1345, 1520, 1595, 1624, 1675, 2362 cm^{-1}. ESI-HRMS (amu): calcd. $C_{31}H_{26}N_4O_7$: 589.1699 [M+Na]; found: 589.1680.

4.2.4.17. (2*Z*)-4-(3*E*,5*E*)-(3,5-Bis-4-nitrobenzylidene-4-oxo-piperidin-1-yl)-4-oxo-but-2-enoic acid (2,4,6-trimethylphenyl)amide (9Bh)

Yellow powder, yield 57%, m.p. 294-297 °C. ^{1}H NMR (500 MHz, DMSO-d_6): δ 2.00 (s, 6H), 2.22 (s, 3H), 4.80 & 4.88 (s, 2H each), 6.14 & 6.46 (d, *J* = 11.5 Hz, 1H each)**,** 6.86 (s, 2H), 7.68 (s, 1H), 7.74 (d, *J* = 8.5 Hz, 2H), 7.78 (s, 1H), 7.83 (d, *J* = 8.5 Hz, 2H), 8.30-8.34 (m, 4H), 9.33 (brs, 1H). ^{13}C NMR (125 MHz, DMSO-d_6): δ 18.4, 20.9, 41.9, 47.3, 124.2, 126.1, 128.7, 131.7, 131.9, 132.3, 133.8, 134.5, 134.6, 135.1, 135.3, 135.7, 136.0, 141.3, 141.4, 147.7, 147.8, 162.1, 167.2, 185.6. UV (λ_{max}, EtOH): 204, 206, 333 nm. IR (ν, KBr): 667, 679, 754, 805, 853, 935, 991, 1109, 1174, 1242, 1276, 1345, 1411, 1436, 1457, 1489, 1521, 1558, 1592, 1616, 1683, 1733, 1772, 2336, 2362, 3646, 3675, 3784, 3853 cm^{-1}. ESI-HRMS (amu): calcd. $C_{33}H_{28}N_4O_7$: 603.1856 [M+Na]; found: 603.1876.

4.2.4.18. (2*Z*)-4-(3*E*,5*E*)-(3,5-Bis-4-nitrobenzylidene-4-oxo-piperidin-1-yl)-4-oxo-but-2-enoic acid (2-ethyl-6-methylphenyl)amide (9Bi)

Yellow powder, yield 72%, m.p. 200-202 °C. ^{1}H NMR (300 MHz, DMSO-d_6): δ 1.01 (t, *J* = 7.5 Hz, 3H), 2.04 (s, 3H), 2.41 (q, *J* = 7.5 Hz 2H), 4.80 & 4.88 (s, 2H each), 6.17 & 6.49 (d, *J* = 11.5 Hz, 1H each)**,** 7.07 (d, *J* = 7.5 Hz, 2H), 7.13 (t, *J* = 7.5 Hz, 1H), 7.69 (s, 1H), 7.73-7.78 (m, 3H), 7.83 (d, *J* = 8.5 Hz, 2H), 8.32 (d, *J* = 8.0 Hz, 4H), 9.43 (brs, 1H). ^{13}C NMR (125 MHz, DMSO-d_6): δ 14.9, 18.6, 24.7, 41.9, 47.3, 124.2, 124.3, 126.0, 126.4, 127.4, 128.1, 131.7, 132.0, 133.8, 134.3, 134.6, 134.9, 135.3, 135.7, 135.9, 141.2, 141.3, 141.4, 147.7, 147.8, 162.4, 167.2, 185.6. UV (λ_{max}, EtOH): 331 nm**.** IR (ν, KBr): 680, 755, 806, 854, 933, 992, 1110, 1172, 1249, 1275, 1344, 1411, 1471, 1520, 1623, 1652, 1733, 2361, 3853 cm^{-1}**.** ESI-HRMS (amu): calcd. $C_{33}H_{28}N_4O_7$: 603.1856 [M+Na]; found: 603.1865.

4.2.4.19. (2*Z*)-4-(3*E*,5*E*)-(3,5-Bis-(4-carboethoxybenzylidene)-4-oxo-piperidin-1-yl)-4-oxo-but-2-enoic acid (2-fluorophenyl)amide (9Ca)

Yellow powder, yield 95%, m.p. 182-183 °C. ^{1}H NMR (500 MHz, DMSO-d_6): δ 1.34-1.37 (m, 6H), 4.32-4.38 (m, 4H), 4.77 & 4.93 (s, 2H each), 6.23 & 6.47 (d, *J* = 11.5 Hz, 1H each), 7.19-7.21 (m, 2H), 7.26-7.31 (m, 1H), 7.40 (d, *J* = 8.0 Hz, 2H), 7.57 (s, 1H), 7.74 (d, *J* = 8.0 Hz, 2H), 7.80 (s, 1H), 7.94-7.97 (m, 3H), 8.07 (d, *J* = 8.0 Hz, 2H), 9.84 (brs, 1H). ^{13}C NMR (125 MHz, DMSO-d_6): δ 14.1, 41.7, 46.6, 60.9, 115.3 (d, *J* = 20 Hz), 123.6, 124.3, 125.3 (d, *J* = 6 Hz), 125.6, 125.7, 125.8, 129.2, 129.4, 129.9, 130.1, 130.2, 130.6, 133.8, 134.1, 135.2, 138.7, 138.6, 153.8 (d, *J* = 245 Hz), 162.0, 165.1, 165.2, 166.4, 185.2. UV (λ_{max}, EtOH): 215, 262, 315 nm. IR (ν, KBr): 750, 773, 858, 937, 1020, 1104, 1186, 1241, 1271, 1414, 1457, 1539, 1622, 1635, 1718, 1733, 3420 cm^{-1}. ESI-HRMS (amu): calcd. $C_{35}H_{31}FN_2O_7$: 633.2013 [M+Na]; found: 633.2005.

4.2.4.20. (2*Z*)-4-(3*E*,5*E*)-(3,5-Bis-(4-carboethoxybenzylidene)-4-oxo-piperidin-1-yl)-4-oxo-but-2-enoic acid (2-chlorophenyl)amide (9Cb)

Yellow powder, yield 92%, m.p. 165-167 °C. ^{1}H NMR (500 MHz, DMSO-d_6): δ 1.33-1.37 (m, 6H), 4.32-4.38 (m, 4H), 4.77 & 4.92 (s, 2H each), 6.27 & 6.50 (d, *J* = 12.0 Hz, 1H each), 7.22 (t, *J* = 7.5 Hz, 1H), 7.36 (t, *J* = 7.5 Hz, 1H), 7.48-7.53 (m, 3H), 7.63 (s, 1H), 7.71-7.78 (m, 4H), 7.99 (d, *J* = 8.0 Hz, 2H), 8.07 (d, *J* = 8.0 Hz, 2H), 9.63 (brs, 1H). ^{13}C NMR (125 MHz, DMSO-d_6): δ 14.6, 42.2, 47.2, 61.4, 126.0, 126.1, 126.3, 127.9, 128.27, 129.8, 130.0, 130.7, 131.1, 134.3, 134.6, 134.7, 134.9, 135.6, 135.7, 139.2, 139.3, 162.5, 165.6, 165.7, 166.9, 185.7. UV (λ_{max}, EtOH): 251, 262, 315 nm. IR (ν, KBr): 526, 645, 752, 773, 803, 859, 937, 996, 1019, 1105, 1183, 1270, 1366, 1413, 1443, 1531, 1622, 1636, 1683, 1719, 3346 cm^{-1}. ESI-HRMS (amu): calcd. $C_{35}H_{31}ClN_2O_7$: 649.1717 [M+Na]; found: 649.1690.

4.2.4.21. (2*Z*)-4-(3*E*,5*E*)-(3,5-Bis-(4-carboethoxybenzylidene)-4-oxo-piperidin-1-yl)-4-oxo-but-2-enoic acid (2-methylphenyl)amide (9Cc) Yellow powder, yield 96%, m.p. 170-171 °C. ^{1}H NMR (500 MHz, DMSO-d_6): δ 1.33-1.37 (m, 6H), 2.14 (s, 3H), 4.32-4.38 (m, 4H), 4.79 & 4.91 (s, 2H each), 6.17 & 6.45 (d, *J* = 12.0 Hz, 1H each), 7.11 (t, *J* = 7.5 Hz, 1H), 7.17-7.24 (m, 2H), 7.42 (d, *J* = 7.5 Hz, 1H), 7.52 (d, *J* = 8.5 Hz, 2H), 7.64 (s, 1H), 7.72 (d, *J* = 8.5 Hz, 2H), 7.77 (s, 1H), 8.05 (d, *J* = 8.0 Hz, 2H), 8.07 (d, *J* = 8.0 Hz, 2H), 9.38 (brs, 1H). ^{13}C NMR (125 MHz, DMSO-d_6): δ 14.1, 17. 8, 41.8, 46.7,

60.9, 124.3, 125.3, 125.9, 126.0, 129.2, 129.3, 130.0, 130.1, 130.2, 130.3, 130.6, 131.2, 133.8, 134.2, 135.1, 135.7, 138.8, 138.9, 161.7, 165.1, 165.2, 166.6, 185.2. UV (λ_{max}, EtOH): 221, 248, 315 nm. IR (ν, KBr): 754, 772, 858, 938, 996, 1018, 1103, 1185, 1239, 1270, 1366, 1413, 1457, 1535, 1621, 1682, 1720, 3384 cm^{-1}. ESI-HRMS (amu): calcd. $C_{36}H_{34}N_2O_7$: 629.2264 [M+Na]; found: 629.2282.

4.2.4.22. (2*Z*)-4-(3*E*,5*E*)-(3,5-Bis-(4-carboethoxybenzylidene)-4-oxo-piperidin-1-yl)-4-oxo-but-2-enoic acid (2-methoxyphenyl)amide (9Cd)

Yellow powder, yield 88%, m.p. 154-156 °C. ^{1}H NMR (500 MHz, DMSO-d_6): δ 1.32-1.37 (m, 6H), 3.84 (s, 3H), 4.32-4.38 (m, 4H), 4.77 & 4.93 (s, 2H each), 6.33 & 6.40 (d, *J* = 11.5 Hz, 1H each), 6.95 (t, *J* = 7.0 Hz, 1H), 7.06-7.14 (m, 2H), 7.39 (d, *J* = 8.0 Hz, 2H), 7.56 (s, 1H), 7.74 (d, *J* = 8.0 Hz, 2H), 7.80 (s, 1H), 7.94 (d, *J* = 8.0 Hz, 2H), 7.98 (d, *J* = 8.0 Hz, 1H), 8.08 (d, *J* = 8.0 Hz, 2H), 9.27 (brs, 1H). ^{13}C NMR (125 MHz, DMSO-d_6): δ 14.6, 42.2, 47.2, 56.1, 61.4, 111.6, 120.7, 122.0, 125.1, 127.1, 127.3, 129.7, 129.9, 130.4, 130.6, 130.7, 131.1, 134.4, 134.6, 135.6, 139.2, 139.4, 149.9, 162.3, 165.7, 167.2, 185.7. UV (λ_{max}, EtOH): 237, 316 nm. IR (ν, KBr): 625, 707, 757, 771, 805, 858, 985, 1021, 1048, 1109, 1171, 1290, 1368, 1410, 1437, 1458, 1485, 1529, 1616, 1684, 1716, 2337, 2362, 2979, 3400 cm^{-1}. ESI-HRMS (amu): calcd. $C_{36}H_{34}N_2O_8$: 645.2213 [M+Na]; found: 645.2188.

4.2.4.23. (2*Z*)-4-(3*E*,5*E*)-(3,5-Bis-(4-carboethoxybenzylidene)-4-oxo-piperidin-1-yl)-4-oxo-but-2-enoic acid (2-nitrophenyl)amide (9Ce)

Yellow powder, yield 93%, m.p. 160-161 °C. ^{1}H NMR (500 MHz, DMSO-d_6): δ 1.35 (t, *J* = 7.0 *Hz*, 6H), 4.35 (q, *J* = 6.5 *Hz*, 4H), 4.75 & 4.90 (s, 2H each), 6.17 & 6.55 (d, *J* = 12.0 Hz, 1H each), 7.42 (t, *J* = 7.5 Hz, 1H), 7.53 (d, *J* = 7.5 Hz, 2H), 7.64 (s, 1H), 7.67-7.77 (m, 5H), 7.99-8.07 (m, 5H), 10.39 (brs, 1H). ^{13}C NMR (125 MHz, DMSO-d_6): δ 14.1, 41.6, 46.6, 60.9, 125.0, 125.1, 125.2, 125.5, 125.6, 129.2, 129.3, 130.0, 130.2, 130.3, 130.6, 130.8, 133.7, 133.8, 134.0, 134.4, 135.2, 135.5, 135.8, 138.6, 138.7, 141.9, 162.0, 165.2, 166.1, 185.1. UV (λ_{max}, EtOH): 217, 249, 330 nm. IR (ν, KBr): 746, 773, 855, 987, 1020, 1106, 1172, 1271, 1334, 1367, 1412, 1457, 1499, 1581, 1608, 1652, 1688, 1720, 2362, 2982, 3327 cm^{-1}. ESI-HRMS (amu): calcd. $C_{35}H_{31}N_3O_9$: 660.1958 [M+Na]; found: 660.1925.

4.2.4.24. (2*Z*)-4-(3*E*,5*E*)-(3,5-Bis-(4-carboethoxybenzylidene)-4-oxo-piperidin-1-yl)-4-oxo-but-2-enoic acid (2,6-dichlorophenyl)amide (9Cf)

Yellow powder, yield 91%, m.p. 176-178 °C. ^{1}H NMR (500 MHz, DMSO-d_6): δ 1.33-1.37 (m, 6H), 4.32-4.38 (m, 4H), 4.77 & 4.87 (s, 2H each), 6.19 & 6.54 (d, *J* = 11.5 Hz, 1H each), 7.37 (t, *J* = 7.0 Hz, 1H), 7.55 (d, *J* = 8.0 Hz, 2H), 7.59 (d, *J* = 8.0 Hz, 2H), 7.66-7.71 (m, 3H), 7.75 (s, 1H), 8.03 (d, *J* = 8.0 Hz, 2H), 8.05 (d, *J* = 8.0 Hz, 2H), 10.11 (brs, 1H). ^{13}C NMR (125 MHz, DMSO-d_6): δ 14.1, 41.4, 46.7, 60.9, 61.0, 124.2, 128.0, 128.5, 129.2, 129.3, 130.1, 130.2, 130.3, 130.6, 132.3, 133.4, 133.6, 133.8, 134.5, 135.1, 135.7, 138.7, 138.8, 161.6, 165.1, 165.2, 166.3, 185.1. UV (λ_{max}, EtOH): 223, 243, 330 nm. IR (ν, KBr): 553, 597, 773, 789, 858, 937, 989, 1019, 1108, 1128, 1183, 1276, 1366, 1412, 1438, 1607, 1634, 1646, 1716, 3282 cm^{-1}. ESI-HRMS (amu): calcd. $C_{35}H_{30}Cl_2N_2O_7$: 683.1328 [M+Na]; found: 683.1311.

4.2.4.25. (2*Z*)-4-(3*E*,5*E*)-(3,5-Bis-(4-carboethoxybenzylidene)-4-oxo-piperidin-1-yl)-4-oxo-but-2-enoic acid (2,6-dimethylphenyl)amide (9Cg)

Yellow powder, yield 91%, m.p. 130-133 °C. ^{1}H NMR (300 MHz, DMSO-d_6): δ 1.32-1.37 (m, 6H), 2.06 (s, 6H), 4.32-4.38 (m, 4H), 4.80 & 4.87 (s, 2H each), 6.16 & 6.47 (d, *J* = 11.5 Hz, 1H each), 7.05-7.10 (m, 3H), 7.60 (d, *J* = 8.0 Hz, 2H), 7.66 (s, 1H), 7.69 (d, *J* = 8.5 Hz, 2H), 7.74 (s, 1H), 8.03-8.06 (m, 4H), 9.45 (brs, 1H). ^{13}C NMR (125 MHz, DMSO-d_6): δ 14.6, 18.5, 41.9, 47.4, 61.4, 61.5, 125.9, 127.0, 128.1, 128.2, 129.8, 129.9, 130.6, 130.7, 130.8, 131.1, 134.3, 134.8, 134.9, 135.0, 135.4, 135.5, 139.2, 162.1, 165.6, 165.7, 167.1, 185.6. UV (λ_{max}, EtOH): 221, 244, 317 nm. IR (ν, KBr): 773, 856, 1019, 1107, 1278, 1367, 1411, 1457, 1559, 1616, 1718, 2336, 2362, 2982, 3629 cm^{-1}. ESI-HRMS (amu): calcd. $C_{37}H_{36}N_2O_7$: 643.2420 [M+Na]; found: 643.2390.

4.2.4.26. (2*Z*)-4-(3*E*,5*E*)-(3,5-Bis-(4-carboethoxybenzylidene)-4-oxo-piperidin-1-yl)-4-oxo-but-2-enoic acid (2,4,6-trimethylphenyl)amide (9Ch)

Yellow powder, yield 90%, m.p. 173-176 °C. ^{1}H NMR (500 MHz, DMSO-d_6): δ 1.31-1.37 (m, 6H), 2.02 (s, 6H), 2.23 (s, 3H), 4.32-4.38 (m, 4H), 4.79 & 4.87 (s, 2H each), 6.14 & 6.45 (d, *J* = 11.5 Hz, 1H each), 6.87 (s, 2H), 7.60 (d, *J* = 8.0 Hz, 2H), 7.66 (s, 1H), 7.69 (d, *J* = 8.0 Hz, 2H), 7.74 (s, 1H), 8.03-8.07 (m, 4H), 9.35 (brs, 1H). ^{13}C NMR (125 MHz, DMSO-d_6): δ 14.6, 18.4, 20.9, 41.9, 47.4, 61.4, 61.5, 125.9, 128.7, 128.9, 129.9, 130.6, 130.7, 130.8, 131.1, 132.3, 134.3, 134.5, 134.7, 134.8, 135.1, 135.5,

136.0, 139.3, 162.1, 165.7, 167.1, 185.6. UV (λ_{max}, EtOH): 219, 241, 331 nm. IR (ν, KBr): 685, 709, 772, 807, 990, 1019, 1105, 1184, 1279, 1367, 1412, 1445, 1521, 1607, 1675, 1724, 2362, 2913, 3240 cm^{-1}. ESI-HRMS (amu): calcd. $C_{38}H_{38}N_2O_7$: 657.2577 [M+Na]; found: 657.2545.

4.2.4.27. (2*Z*)-4-(3*E*,5*E*)-(3,5-Bis-(4-carboethoxybenzylidene)-4-oxo-piperidin-1-yl)-4-oxo-but-2-enoic acid (2-ethyl-6-methylphenyl)amide (9Ci)

Yellow powder, yield 82%, m.p. 166-169 °C. ^{1}H NMR (500 MHz, DMSO-d_6): δ 1.03 (t, *J* = 6.5 *Hz*, 3H), 1.31-1.36 (m, 6H), 2.05 (s, 3H), 2.41-2.44 (m, 2H), 4.33-4.37 (m, 4H), 4.79 & 4.87 (s, 2H each), 6.18 & 6.48 (d, *J* = 11.5 Hz, 1H each), 7.06-7.14 (m, 3H), 7.59-7.80 (m, 6H), 8.05 (m, 4H), 9.45 (brs, 1H). ^{13}C NMR (125 MHz, DMSO-d_6): δ 14.6, 14.9, 18.6, 24.7, 41.9, 47.3, 61.4, 61.5, 125.8, 126.4, 127.4, 128.1, 129.8, 129.9, 130.6, 130.7, 130.8, 131.1, 134.2, 134.3, 134.5, 134.8, 134.9, 135.5, 135.9, 139.3, 141.2, 162.5, 165.7, 167.1, 185.7. UV (λ_{max}, EtOH): 219, 244, 327 nm. IR (ν, KBr): 772, 809, 855, 935, 1019, 1104, 1186, 1279, 1367, 1412, 1445, 1521, 1607, 1725, 2977, 3231 cm^{-1}. ESI-HRMS (amu): calcd. $C_{38}H_{38}N_2O_7$: 657.2577 [M+Na]; found: 657.2582.

4.3. Biological evaluations

4.3.1. Cytostatic activity

The compounds were evaluated in the Molt 4/C8, CEM and L1210 screens using a reported procedure [34]. In brief, various concentrations of compounds in suitable solvents were incubated at 37 ^{o}C with Molt 4/C8, CEM and L1210 cells and the percentage survival was noted at the end of 48h. Control experiments in which the compounds were omitted were also undertaken. All test and control tests were carried out in triplicate at each concentration of the compound and the data is collated in Table 1. The human tumor cell line screen at the National Cancer Institute (NCI) was undertaken by a reported procedure [35] using 57 or 59 tumor cell lines. The data are summarized in Table 2.

4.3.2. Culture of human fibroblasts

WI-38 cells or human fibroblasts (ATCC® CCL-75™) were obtained from Cederlane labs (Burlington, ON, Canada) and cultured according to the supplier's instructions. The cells were cultured using DMEM medium, supplemented with 10%

FBS and 100 mg/L of penicillin and streptomycin. The cultures were maintained in 75 cm^2 culture flasks at a steady temperature of 37°C in a humidified incubator (VWR International, Mississauga, ON) and the growth medium of cultured cells was changed every 48 h.

4.3.3. Topoisomerase IIα assays

All test compounds were assayed at 50 μM concentration using a commercial kit, (Catalog no: TG1001-2; Topogen Inc, Columbus, OH). The assay is based upon evaluating the formation of DNA cleavage products, primarily linearized DNA (interfacial poisons) and/or supercoiled product (catalytic inhibitory compounds). All the preparatory and analysis steps were performed according to the manufacturer's instructions and then stained using Gel red nucleic acid dye (VWR, ON, Canada).

4.3.4. Antioxidant assays

4.3.4.1. Ferric reducing ability of a plasma (FRAP) assay

The FRAP analysis was performed according to our recent reports [15, 33]. The anti-oxidant capacity results were expressed as μM TE L^{-1} of solution (Table 3).

4.3.4.2. Oxygen radical absorbance capacity (ORAC) assay

The ORAC analysis was performed according to our recent reports [15, 33]. The anti-oxidant capacity results were expressed as μM TE L^{-1} of solution (Table 3).

4.3.4.3. The 2,2-diphenylpicrylhydrazyl (DPPH) assay

The DPPH antioxidant assay was performed according to our recent reports [15, 33]. The anti-oxidant capacity results were expressed as %inhibition of DPPH radical with respect to untreated control (Table 3).

4.3.4.4. Cellular reactive oxygen species (ROS) detection assay

ROS inhibition by curcumin inspired compounds in WI-38 cells by using the dichlorofluorescein (DCF) assay according to the detailed method described in our recent report [33]. The results were expressed as percentage inhibition of ROS with respect to an assay control (Table 3).

4.3.5. In-vitro toxicity assays

Two *in vitro* toxicity analyses were conducted using the CytoTox-ONE™ homogeneous membrane integrity LDH and CellTiter 96® AQ_{ueous} non-radioactive cell proliferation MTS assay (Promega Corporation, Madison, WI). The experiments were

performed using WI-38 cells and results depicting the cell survival and membrane damage in cells were calculated with respect to the positive control cells (Table 4).

4.3.6. In-vivo neurotoxicity assays

Twenty nine compounds (**4C, 9Aa-g, 9Ai, 9Ba-i, 9Cb, 9cd** and **11a-i**) were examined for murine toxicity using a reported procedure [42]. In brief, the compounds were administered to mice by the intraperitoneal route using doses of 30, 100 and 300 mg/kg. The animals were observed after 0.5 and 4 h. Neurotoxicity, which was determined by the rotarod method,[42] was observed after administration of the test compounds. The results are presented in Table 5. The Anticonvulsant Screening Program of the National Institute of Neurological Disorders and Stroke, USA requires that all mice be housed, fed and handled in ways which are consistent with the recommendations of the National Research Council Publication 'Guide for the Care and Use of Laboratory Animals'. All mice were euthanized in accordance with the policies of the Institute of Laboratory Resources dealing with the humane care of laboratory animals.

4.4. Statistical analyses

Chem3D® computer program was used to calculate atomic charges (charge β_1 and charge β_2), the molar refractivity values (MR_{mol}) and the calculated partition coefficient (logP) of series **9A-C** compounds.[22] Briefly, the energy of the molecular structure of the compound was minimized using Merck Molecular Force Field (MMFF94). Atomic charges were obtained using extended Hückel method. MR_{mol} and logP was calculated using ChemPropPro engine. The E_s, π and molar refractivity (MR_{sub}) values of the aryl substituents in series **9A-C** were obtained from the literature [44]. The linear and semilogarithmic correlations were obtained using a commercial software package [42]. Significant correlations and trends towards significance obtained are summarized in Table 6.

Acknowledgements

The following sources of financial support for this study are gratefully acknowledged: Nova Scotia Health Research Foundation (to AJ) and Natural Sciences and Engineering Research Council of Canada (to AJ and HPVR), the Canada Research Chair program (to

HPVR), Belgian Fonds voor Geneeskundig Wetenschappelik Onderzoek (to JB), Pfizer Summer Undergraduate Research Fellowship (to KD and MN). Appreciation is extended to Mrs. Lizette van Berckelaer for conducting the Molt 4/C8, CEM and L1210 assays, the National Cancer Institute (NCI), U.S.A., which provided the data using the panel of human tumor cell lines and the National Institute of Neurological Disorders and Stroke (NINDS), U.S.A. for undertaking the short-term toxicity studies in mice.

Supplementary data

Supplementary data (characterization data for new compounds) associated with this article can be found, in the online version, at http://dx.doi.org/10.1016/j.bmc.2015.????.

.

References

[1] B.B. Aggarwal, C. Sundaram, N. Malani, H. Ichikawa, Curcumin: the Indian solid gold, The molecular targets and therapeutic uses of curcumin in health and disease, Springer2007, pp. 1-75.
[2] S. Julie, M. Jurenka, Anti-inflammatory properties of curcumin, a major constituent: A review of preclinical and clinical research, Altern. Med. Rev., 14 (2009) 141-153.
[3] M.-C. Perry, M. Demeule, A. Régina, R. Moumdjian, R. Béliveau, Curcumin inhibits tumor growth and angiogenesis in glioblastoma xenografts, Mol. Nutr. Food Res., 54 (2010) 1192-1201.
[4] Y.-K. Lee, S.Y. Park, Y.-M. Kim, O.J. Park, Regulatory Effect of the AMPK–COX-2 Signaling Pathway in Curcumin-Induced Apoptosis in HT-29 Colon Cancer Cells, Ann. NY Acad. Sci. , 1171 (2009) 489-494.
[5] C.-L. Yang, Y.-Y. Liu, Y.-G. Ma, Y.-X. Xue, D.-G. Liu, Y. Ren, X.-B. Liu, Y. Li, Z. Li, Curcumin blocks small cell lung cancer cells migration, invasion, angiogenesis, cell cycle and neoplasia through Janus kinase-STAT3 signalling pathway, PLoS One, 7 (2012) e37960.
[6] B.B. Aggarwal, Y.-J. Surh, S. Shishodia, The molecular targets and therapeutic uses of curcumin in health and disease, Springer2007.
[7] National Institutes of Health. http://clinicaltrials.gov/ct2/results?term=curcumin&pg=1 (last accessed May 29, 2015).
[8] M. Bayet-Robert, F. Kwiatkowski, M. Leheurteur, F. Gachon, E. Planchat, C. Abrial, M.A. Mouret-Reynier, X. Durando, C. Barthomeuf, P. Chollet, Phase I dose escalation trial of docetaxel plus curcumin in patients with advanced and metastatic breast cancer, Cancer Biol. Ther., 9 (2010) 8-14.
[9] S.H. Sun, H.C. Huang, C. Huang, J.K. Lin, Cycle arrest and apoptosis in MDA-MB-231/Her2 cells induced by curcumin, Eur. J. Pharmacol., 690 (2012) 22-30.
[10] R. Epelbaum, M. Schaffer, B. Vizel, V. Badmaev, G. Bar-Sela, Curcumin and gemcitabine in patients with advanced pancreatic cancer, Nutr. Cancer, 62 (2010) 1137-1141.

[11] C.H. Goss, A. Genatossio, R.K. Rowbotham, N. Hemblett, S. McNamara, M. Knowles, L. Brass-Ernst, M.L. Aitken, P.L. Zeitlin, M.P. Boyle, A Phase I safety and dose finding study of orally administered curcuminoids in adult subjects with cystic fibrosis who are homozygous for delta F508 cystic fibrosis transmembrane conductance regulator (ΔF508 CFTR) (Abstract # 247), Ped. Pulmonol. , 41 (Suppl.) (2006) 293.
[12] R.A. Taylor, M.C. Leonard, Curcumin for inflammatory bowel disease: a review of human studies, Altern. Med. Rev., 16 (2011) 152-156.
[13] B.J. Kelley, D.S. Knopman, Alternative medicine and Alzheimer disease, Neurologist, 14 (2008) 299-306.
[14] R.A. Sharma, W.P. Steward, A.J. Gescher, Pharmacokinetics and pharmacodynamics of curcumin, in: B. Aggarwal, Y.-J. Surh, S. Shishodia (Eds.) The Molecular Targets and Therapeutic Uses of Curcumin in Health and Disease, Springer US2007, pp. 453-470.
[15] K. Bhullar, A. Jha, D. Youssef, H.P.V. Rupasinghe, Curcumin and its carbocyclic analogs: Structure-activity in relation to antioxidant and selected biological properties, Molecules, 18 (2013) 5389-5404.
[16] A. Jha, J. Zhao, T. Stanley Cameron, E. De Clercq, J. Balzarini, E.K. Manavathu, J.P. Stables, Design, synthesis and biological evaluation of novel curcumin analogues as anti-neoplastic agents, Lett. Drug Des. Discovery, 3 (2006) 304-310.
[17] C.E. Nichols, D. Youssef, R.G. Harris, A. Jha, Microwave-assisted synthesis of curcumin analogs, Arkivoc, 13 (2006) 64-72.
[18] D. Youssef, C.E. Nichols, T.S. Cameron, J. Balzarini, E. De Clercq, A. Jha, Design, synthesis, and cytostatic activity of novel cyclic curcumin analogues, Bioorg. Med. Chem. Lett., 17 (2007) 5624-5629.
[19] J.R. Dimmock, A. Jha, G.A. Zello, J.W. Quail, E.O. Oloo, K.H. Nienaber, E.S. Kowalczyk, T.M. Allen, C.L. Santos, E. De Clercq, J. Balzarini, E.K. Manavathu, J.P. Stables, Cytotoxic N-[4-(3-aryl-3-oxo-1-propenyl)phenylcarbonyl]-3,5-bis(phenylmethylene)-4-piperidones and related compounds, Eur. J. Med. Chem., 37 (2002) 961-972.
[20] A. Jha, C. Mukherjee, A.K. Prasad, V.S. Parmar, E.D. Clercq, J. Balzarini, J.P. Stables, E.K. Manavathu, A. Shrivastav, R.K. Sharma, K.H. Nienaber, G.A. Zello, J.R. Dimmock, E,E,E-1-(4-Arylamino-4-oxo-2-butenoyl)-3,5-bis(arylidene)-4-piperidones: A topographical study of some novel potent cytotoxins, Bioorg. Med. Chem., 15 (2007) 5854-5865.
[21] J.R. Dimmock, A. Jha, G.A. Zello, R.K. Sharma, A. Shrivastav, P. Selvakumar, T.M. Allen, C.L. Santos, J. Balzarini, E. De Clercq, E.K. Manavathu, J.P. Stables, 3,5-Bis(Phenylmethylene)-1-(N-arylmaleamoyl)-4-piperidones: A Novel Group of Cytotoxic Agents, J. Enzyme Inhib. Med. Chem., 18 (2003) 325-332.
[22] D. Youssef, E. Potter, M. Jha, E. De Clercq, J. Balzarini, J.P. Stables, A. Jha, Design, synthesis and bioevaluation of novel maleamic amino acid ester conjugates of 3,5-bisarylmethylene-4-piperidones as cytostatic agents, Bioorg. Med. Chem. Lett., 19 (2009) 6364-6367.
[23] A. Jha, J.R. Dimmock, Syntheses of 4-(3,5-Bisphenylmethylene-4-oxo-piperidin-1-yl)-4-oxo-but-2 Z -enoic Acid Arylamides as Candidate Cytotoxic Agents, Synth. Commun., 33 (2003) 1211-1223.

[24] A. Jha, K.M. Duffield, 3, 5-Bis(arylmethylene)-4-piperidone derivatives as novel anticancer agents, Indian J. Chem., Sect. B: Org. Chem. Incl. Med. Chem., 45 (2006) 2313-2320.
[25] A. Jha, C. Mukherjee, A.J. Rolle, E. De Clercq, J. Balzarini, J.P. Stables, Cytostatic activity of novel 4′-aminochalcone-based imides, Bioorg. Med. Chem. Lett., 17 (2007) 4545-4550.
[26] V. Parmar, S. Jain, K. Bisht, N.K. Sharma, S. Gupta, A.K. Prasad, A. Jha, S. Malhotra, S.K. Sharma, M. Bracke, Synthesis and anti-invasive activity of novel 1, 3-diarylpropenones, Indian J. Chem., Sect. B: Org. Chem. Incl. Med. Chem., (1999) 628-643.
[27] J.R. Dimmock, A. Jha, G.A. Zello, T.M. Allen, C.L. Santos, J. Balzarini, E. De Clercq, E.K. Manavathu, J.P. Stables, Cytotoxic 4-aminochalcones and related compounds, Die Pharmazie-An International Journal of Pharmaceutical Sciences, 58 (2003) 227-232.
[28] A. Jha, C. Mukherjee, A.K. Prasad, V.S. Parmar, M. Vadaparti, U. Das, E. De Clercq, J. Balzarini, J.P. Stables, A. Shrivastav, R.K. Sharma, J.R. Dimmock, Derivatives of aryl amines containing the cytotoxic 1,4-dioxo-2-butenyl pharmacophore, Bioorg. Med. Chem. Lett., 20 (2010) 1510-1515.
[29] A.K. McClendon, N. Osheroff, DNA topoisomerase II, genotoxicity, and cancer, Mutat. Res., 623 (2007) 83-97.
[30] J.E. Deweese, N. Osheroff, The DNA cleavage reaction of topoisomerase II: wolf in sheep's clothing, Nucleic Acids Res., 37 (2009) 738-748.
[31] D.A. Burden, N. Osheroff, Mechanism of action of eukaryotic topoisomerase II and drugs targeted to the enzyme, BBA - Gene Struc. Expr., 1400 (1998) 139-154.
[32] Y. Pommier, Drugging Topoisomerases: Lessons and Challenges, ACS Chem. Biol., 8 (2013) 82-95.
[33] N.K. Paul, M. Jha, K.S. Bhullar, H.P. Vasantha Rupasinghe, J. Balzarini, A. Jha, All trans 1-(3-arylacryloyl)-3,5-bis(pyridin-4-ylmethylene)piperidin-4-ones as curcumin-inspired antineoplastics, Eur. J. Med. Chem., 87 467-470.
[34] J. Balzarini, E. De Clercq, M.P. Mertes, D. Shugar, P.F. Torrence, 5-Substituted 2′-deoxyuridines: Correlation between inhibition of tumor cell growth and inhibition of thymidine kinase and thymidylate synthetase, Biochem. Pharmacol., 31 (1982) 3673-3682.
[35] M.R. Boyd, K.D. Paull, Some practical considerations and applications of the National Cancer Institute in vitro anticancer drug discovery screen, Drug Dev. Res., 34 (1995) 91-109.
[36] J.R. Dimmock, M.P. Padmanilayam, R.N. Puthucode, A.J. Nazarali, N.L. Motaganahalli, G.A. Zello, J.W. Quail, E.O. Oloo, H.-B. Kraatz, J.S. Prisciak, T.M. Allen, C.L. Santos, J. Balzarini, E. De Clercq, E.K. Manavathu, A Conformational and Structure−Activity Relationship Study of Cytotoxic 3,5-Bis(arylidene)-4-piperidones and Related N-Acryloyl Analogues, J. Med. Chem., 44 (2001) 586-593.
[37] A.M. Whittle, S. Feyler, D.T. Bowen, Durable second complete remissions with oral melphalan in hypocellular Acute Myeloid Leukemia and Refractory Anemia with Excess Blast with normal karyotype relapsing after intensive chemotherapy, Leukemia Res. Rep., 2 (2013) 9-11.

[38] R.M. Linka, A.C.G. Porter, A. Volkov, C. Mielke, F. Boege, M.O. Christensen, C-Terminal regions of topoisomerase IIα and IIβ determine isoform-specific functioning of the enzymes in vivo, Nucl. Acids Res., 35 (2007) 3810-3822.
[39] S.V.G. Nair, Ziaullah, H.P.V. Rupasinghe, Fatty acid esters of phloridzin induce apoptosis of human liver cancer cells through altered gene expression, PLoS One, 9 (2014) e107149.
[40] E. Potter, M. Jha, K.S. Bhullar, H.P.V. Rupasinghe, J. Balzarini, A. Jha, Investigation of fatty acid conjugates of 3,5-bisarylmethylene-4-piperidone derivatives as antitumor agents and human topoisomerase-IIα inhibitors, Bioorg. Med. Chem., 23 (2015) 411-421.
[41] H.J. Shen, Y.H. Wang, J. Xu, [Suppression of the growth of subcutaneous transplanted human liver cancer and lung metastasis in nude mice treated by sorafenib combined with fluorouracil], Zhonghua zhong liu za zhi [Chinese journal of oncology], 35 (2013) 98-102.
[42] J.P. Stables, H.J. Kupferberg, The NIH Anticonvulsant Drug Development (ADD) Program: preclinical anticonvulsant, 1997.
[43] Charge β, partition coefficients (LogP) and molar refractivity (MRmol) were calculated by Chem3D® computer program (version 8.0) after energy minimization of the molecules using MOPAC. Chem3D® is obtainable from Cambridge Soft Corporation, Cambridge, MA, USA.
[44] C. Hansch, A. Leo, D. Hoekman, S.R. Heller, Exploring Qsar, American Chemical Society Washington, DC1995.
[45] Minitab® Release 14 obtained from Minitab Inc., Quality Plaza, 1829 Pine Hall Road, State College, PA 16801-3008, USA.
[46] P. Lagisetty, D.R. Powell, V. Awasthi, Synthesis and structural determination of 3,5-bis(2-fluorobenzylidene)-4-piperidone analogs of curcumin, J. Mol. Struct., 936 (2009) 23-28.
[47] J.M. Barrales-Rienda, J.G. Ramos, M.S. Chavez, Synthesis of N-(fluorophenyl)maleamic acids and N-(fluorophenyl)maleimides, J. Fluorine Chem., 9 (1977) 293-308.
[48] L. Canoira, J.G. Rodriguez, Synthesis of oxindole derivatives from N-alkenyl-o-chloroanilides with zero-valent nickel complex, J. Heterocycl. Chem., 22 (1985) 1511-1518.
[49] V.O.T. Omuaru, Reactions of cyclic anhydrides with aromatic primary amines: Part 3 - Synthesis of novel 3-(N-arylcarbamoyl)- and 3-(N-naphthylcarbamoyl)carboxylic acids. Indian J. Chem. Sec. B Org. Chem. Incl. Med. Chem., 37 (1998) 814-816.
[50] S.B. Wagh, P. Balasubramaniyan, V. Balasubramaniyan, Reactions of cyclic anhydrides: Part VII - Reductive cyclisation of 2-nitromaleanilates and 2-nitrofumaranilates, a new synthesis of 2-oxo-1,2,3,4-tetrahydroquinoxalines, Indian J. Chem. Sec. B Org. Chem. Incl. Med. Chem., 21 (1982) 1071-1073.
[51] R.J. Rahaim Jr, R.E. Maleczka Jr, Palladium-Catalyzed Silane/Siloxane Reductions in the One-Pot Conversion of Nitro Compounds into Their Amines, Hydroxylamines, Amides, Sulfonamides, and Carbamates, Synthesis, 2006 (2006) E1-E1.
[52] N. Salewska, M.J. Milewska, Efficient Method for the Synthesis of Functionalized Basic Maleimides, J. Heterocycl. Chem., 51 (2014) 999-1003.

Graphical Abstract:

Curcumin-inspired cytotoxic 3,5-bis(arylmethylene)-1-(*N*--(*ortho*-substituted aryl)maleamoyl)-4-piperidones: A novel Group of topoisomerase II alpha inhibitors

Amitabh Jha,* Katherine M. Duffield, Matthew R. Ness, Sujatha Ravoori, Gabrielle Andrews, Khushwant S. Bhullar, H.P. Vasantha Rupasinghe and Jan Balzarini